SUPPLEMENTAL DATA

Epigenetic reprogramming induced by chronic TCR stimulation unmasks targetable NK receptor signaling in peripheral T-cell lymphomas

Sylvain Carras[1,2,3], Dimitri Chartoire[1,2,3], Sylvain Mareschal[1,2,3], Maël Heiblig[1,2,3], Antoine Marçais[5], Rémy Robinot[1,2,3], Mirjam Urb[1,2,3], Roxane Pommier[6] , Edith Julia[1,2,3], Amel Chebel[1,2,3], Aurélie Verney[1,2,3], Charlotte Bertheau[7], Emilie Bardel[1,2,3], Caroline Fezelot[1,2,3], Lucien Courtois[1,2,3], Camille Lours[1,2,3], Alyssa Bouska[8], Sharma Sunandini[8], Christine Lefebvre[9,10], Jean-Pierre Rouault[1,2,3], David Sibon[11], Anthony Ferrari[6], Javeed Iqbal[8], Laurence de Leval[12], Philippe Gaulard[13,14], Alexandra Traverse-Glehen[1,2,3,7], Pierre Sujobert[1,2,3,4], Mathieu Blery[16], Gilles Salles[1,2,3,4], Thierry Walzer[5], Emmanuel Bachy[1,2,3,4] and Laurent Genestier[1,2,3]

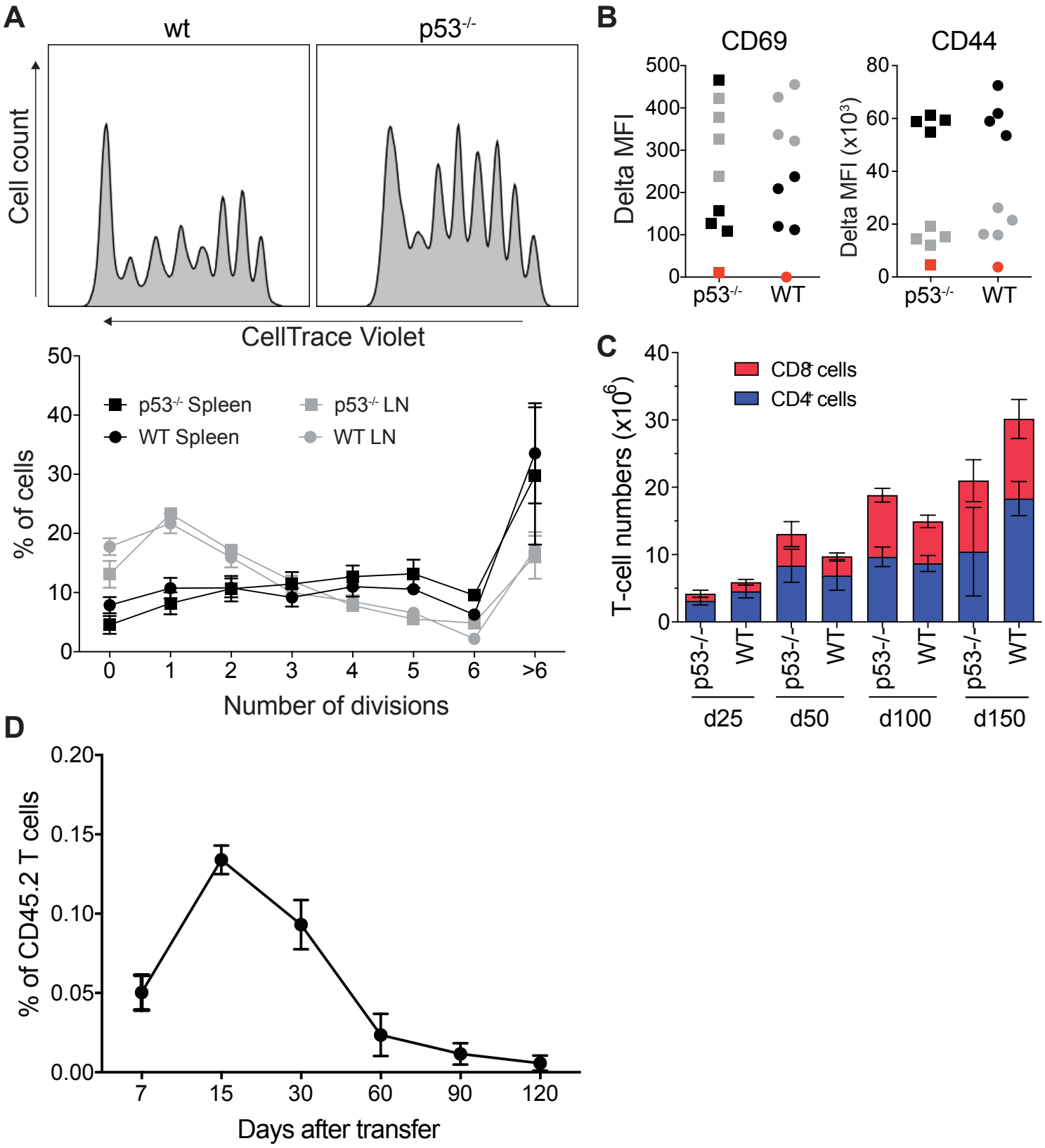

SUPPLEMENTAL FIGURE 1

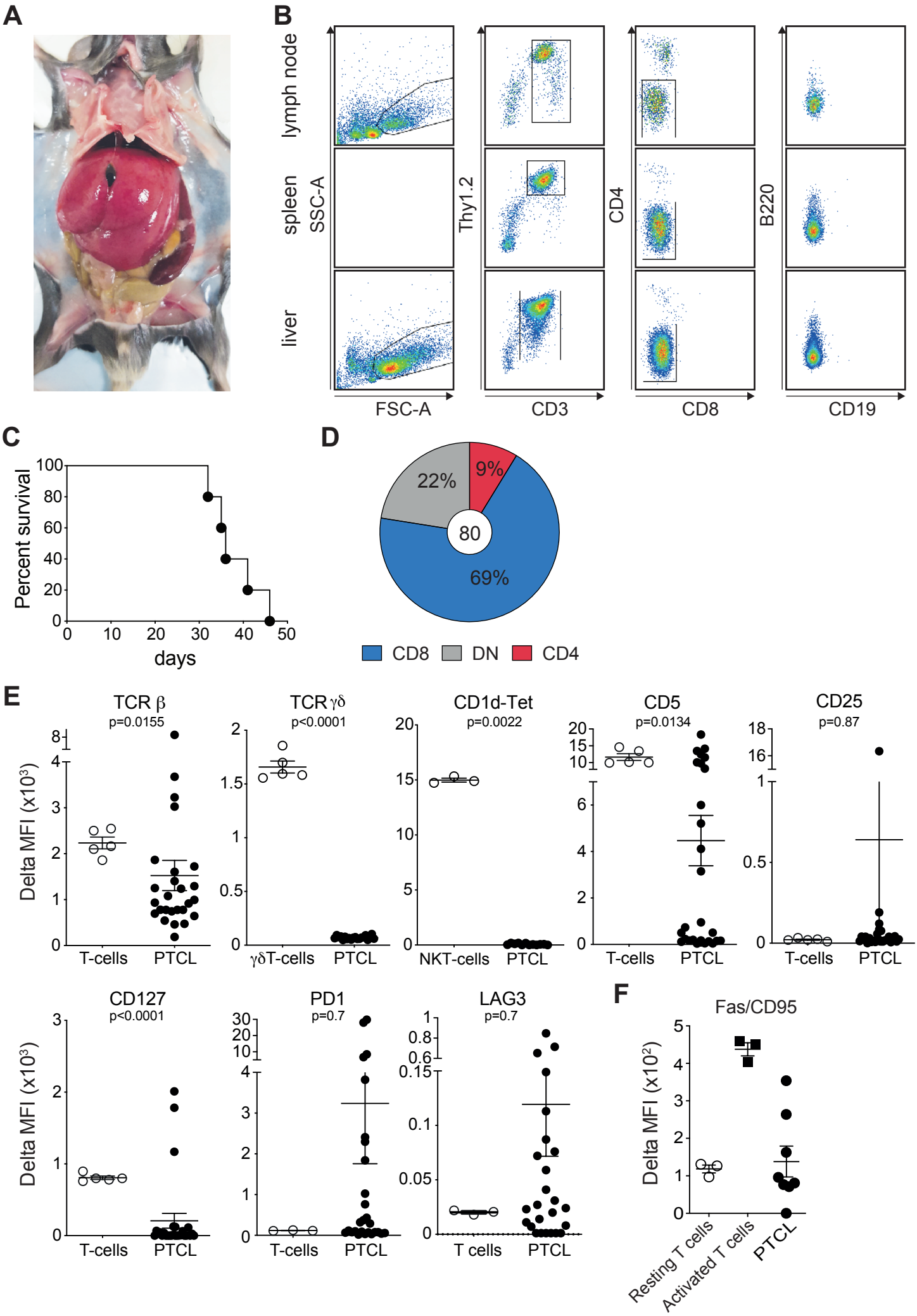

SUPPLEMENTAL FIGURE 2

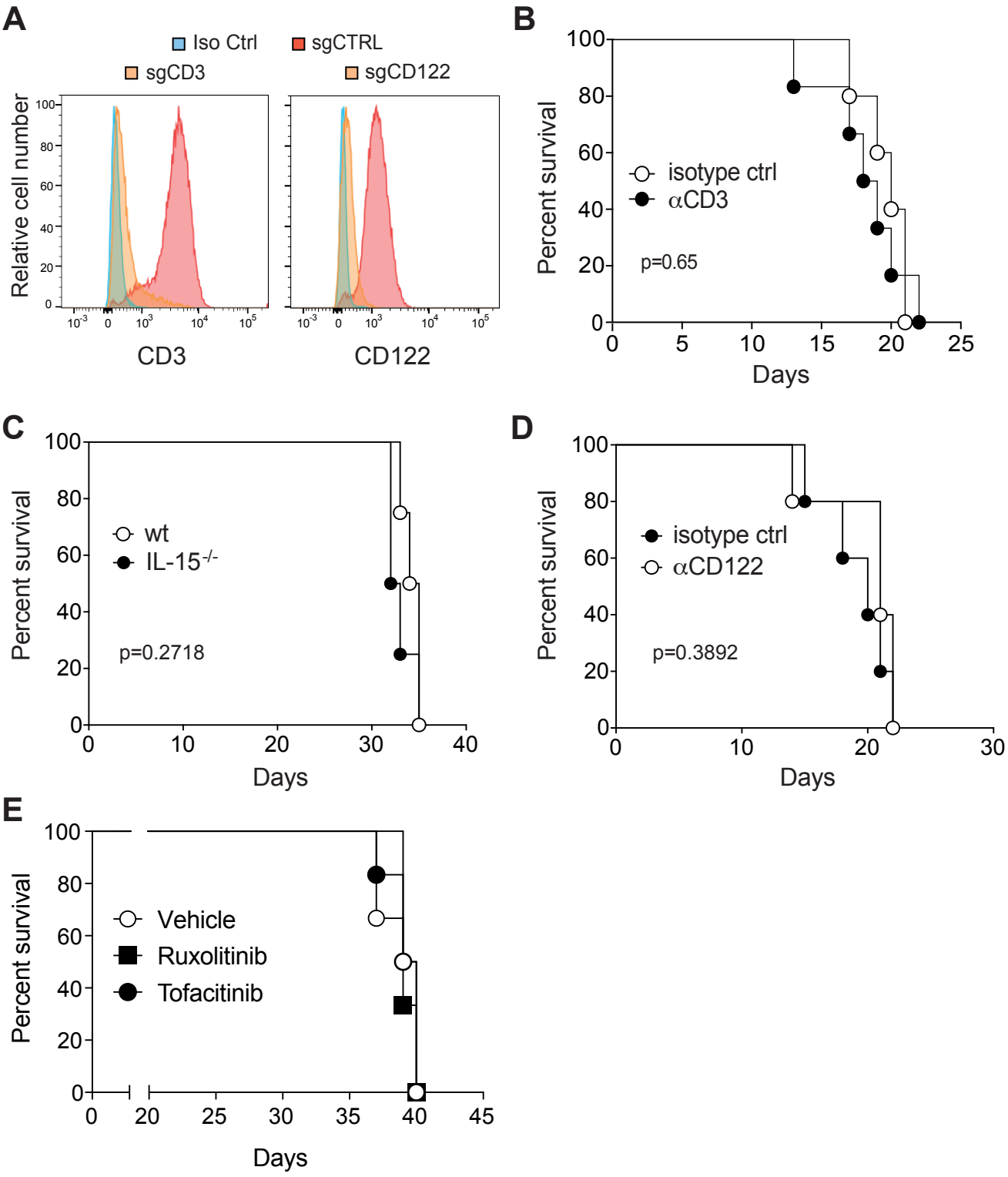

SUPPLEMENTAL FIGURE 3

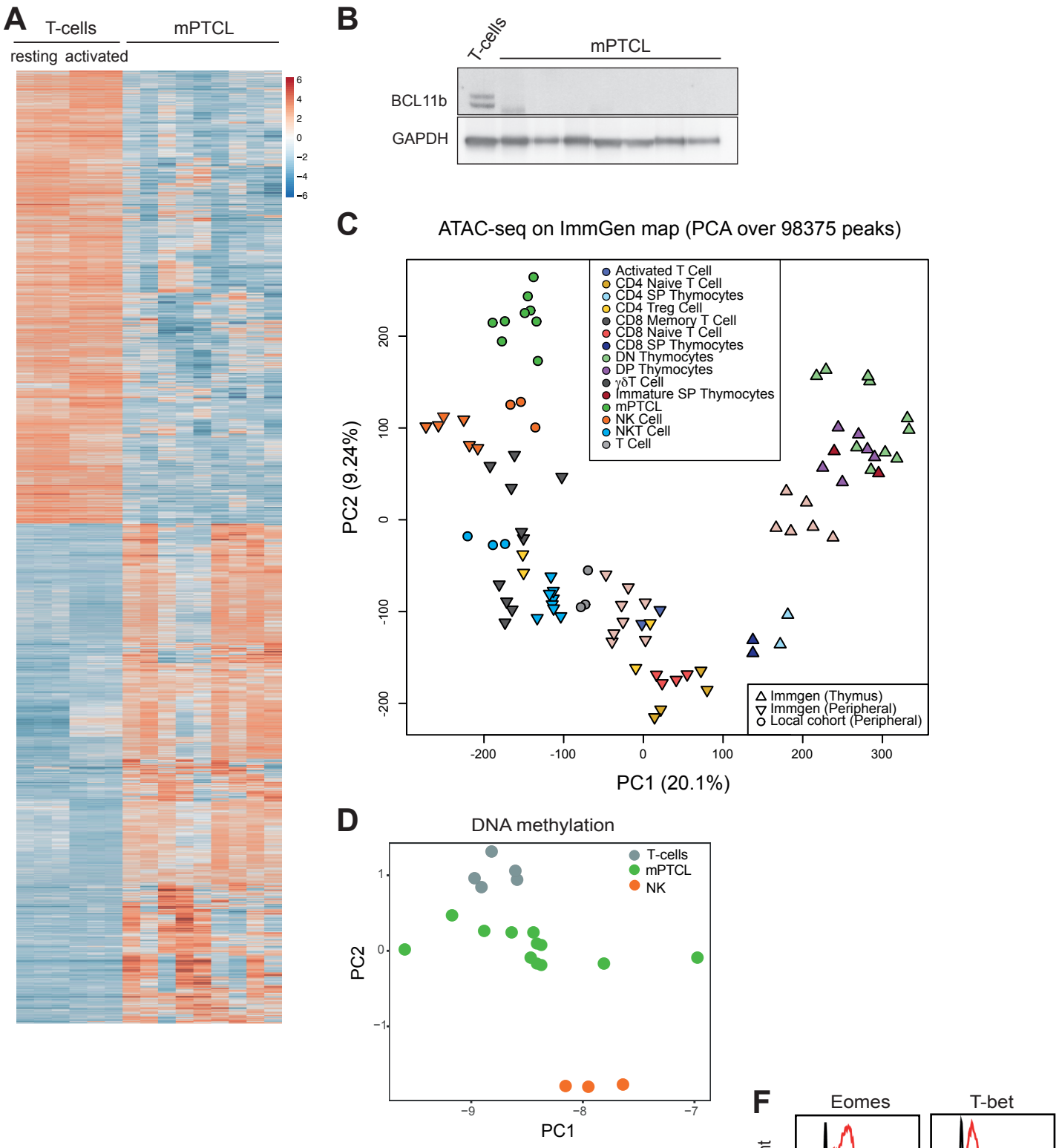

SUPPLEMENTAL FIGURE 4

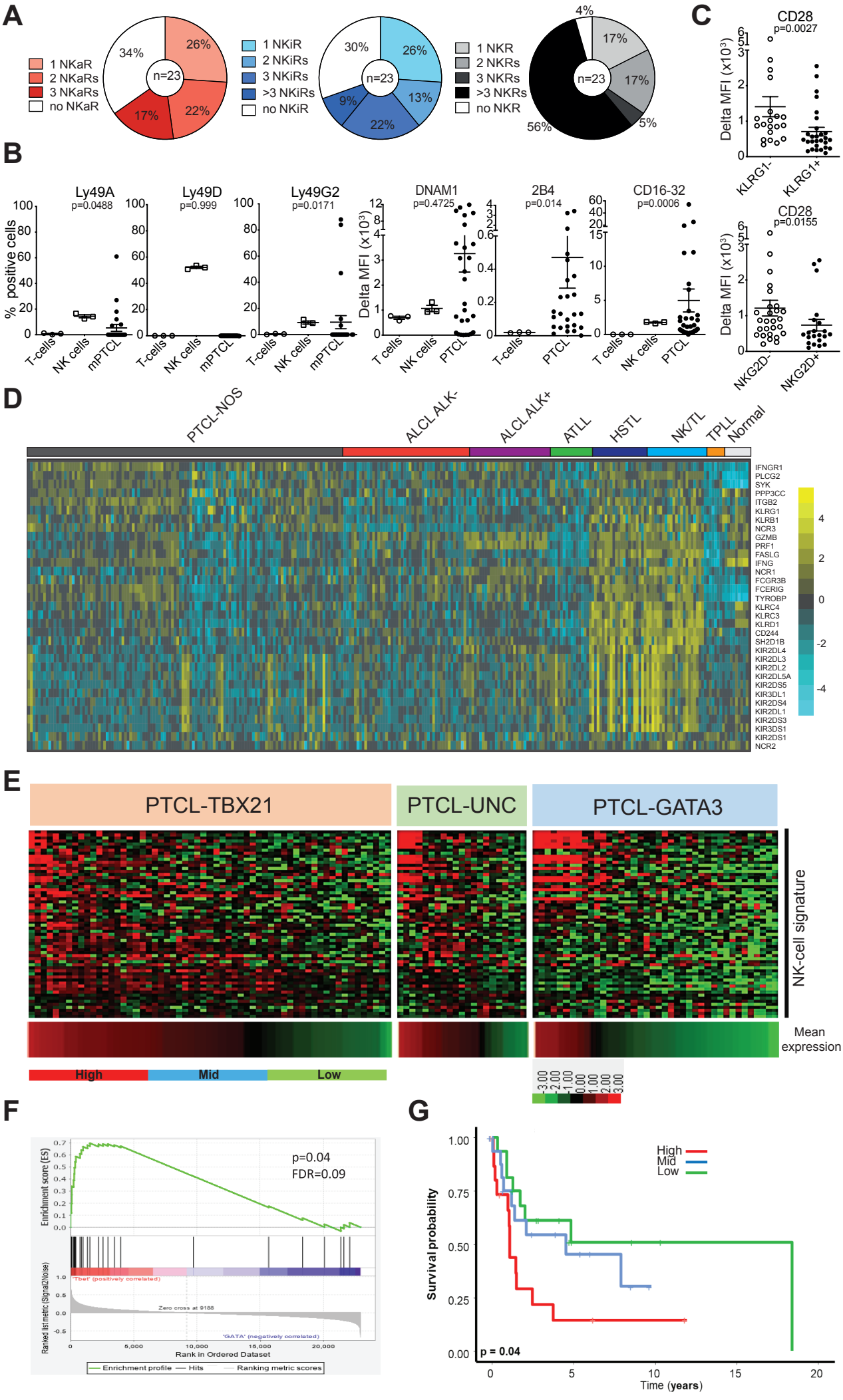

SUPPLEMENTAL FIGURE 5

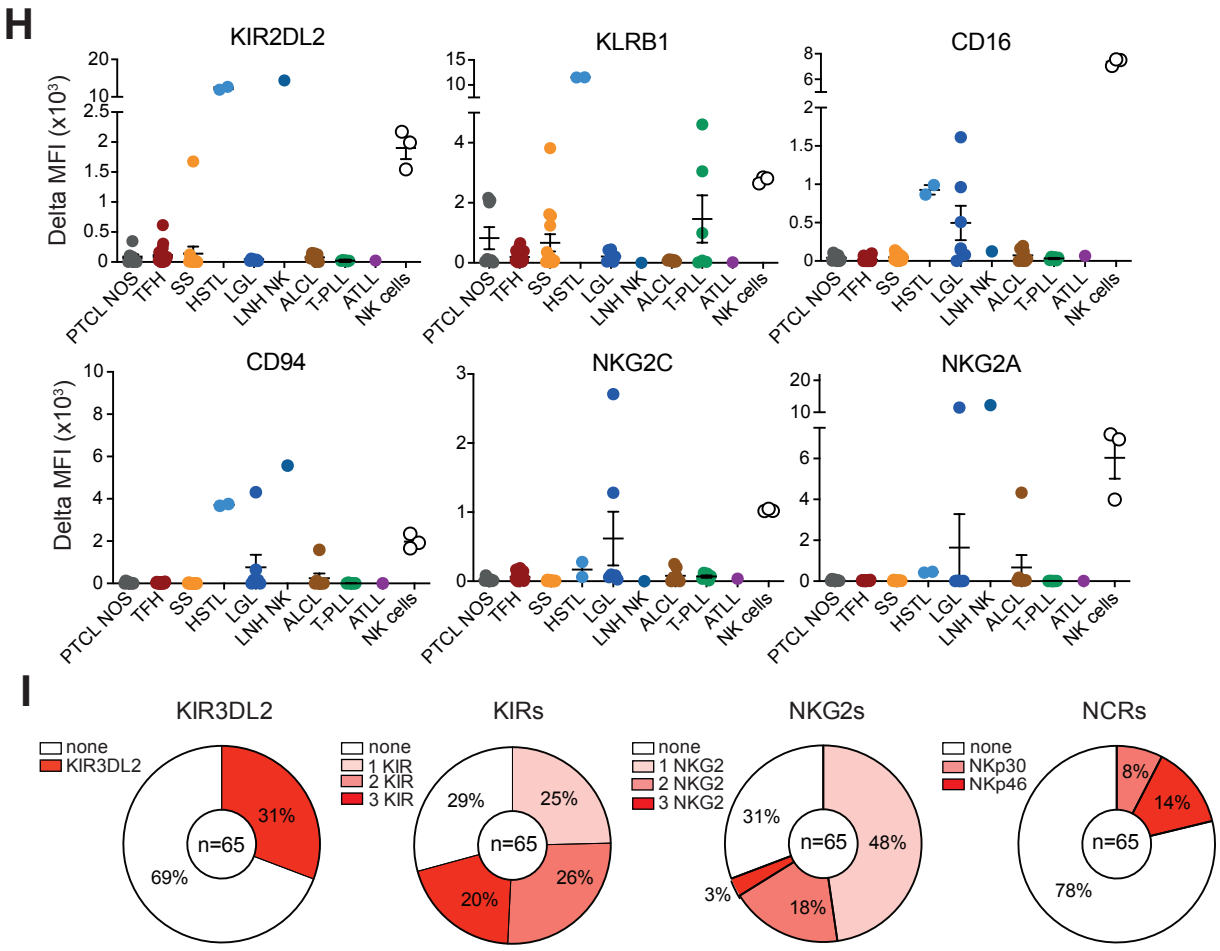

SUPPLEMENTAL FIGURE 5 Continue

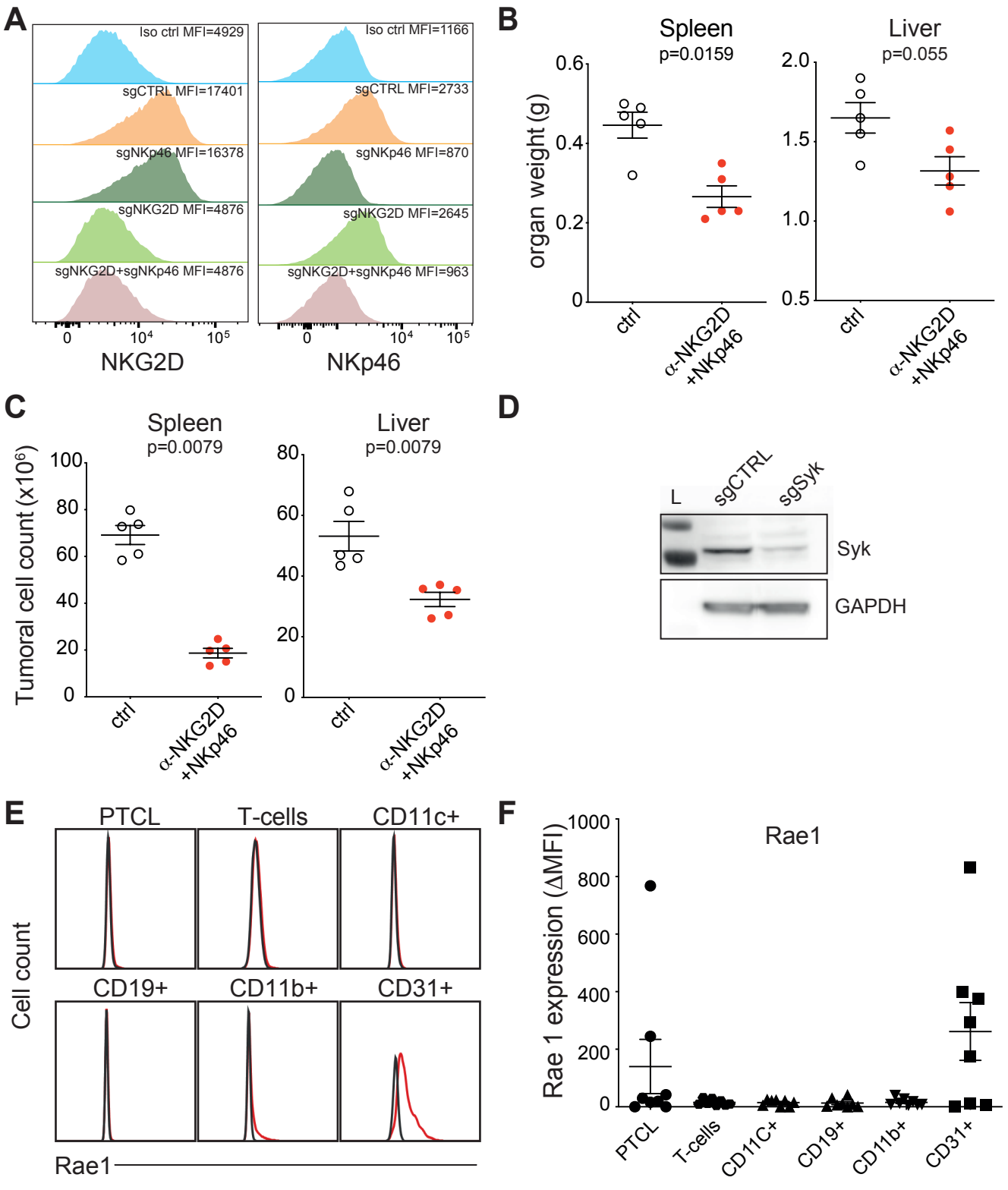

SUPPLEMENTAL FIGURE 6

SUPPLEMENTAL FIGURE LEGENDS

Supplemental Figure 1: Characterization of homeostatic proliferation. (**A**) *In vivo* CellTrace violet (CTV) proliferation assay of WT and *p53*$^{-/-}$ T cells isolated from spleens 5 days after transfer into *CD3*ε$^{-/-}$ mice and distribution of cell division number in WT and *p53*$^{-/-}$ T cells harvested from lymph nodes and spleen of recipient mice. (**B**) Scatter plot representation of CD69 and CD44 expression in WT and *p53*$^{-/-}$ T cells before transfer (red symbols) or harvested from lymph nodes (grey symbols) and spleen (black symbols) 5 days after transfer into *CD3*ε$^{-/-}$ mice. (**C**) CD4 and CD8 absolute cell counts in *CD3*ε$^{-/-}$ mice transferred with WT or *p53*$^{-/-}$ T cells at different time points (n=3/group and timepoints). (**D**) Percentages of CD45.2 *p53*$^{-/-}$ T cells after transfer into CD45.1 WT recipient mice.

Supplemental Figure 2: Macroscopic and phenotypic characterization of mPTCLs. (A) Macroscopic characteristic of a PTCL-bearing mouse showing hepatosplenomegaly. **(B)** Representative gating strategy and lymphoma cell infiltration in liver, spleen and lymph nodes of a single mPTCL. **(C)** Survival curve of syngeneic C57BL6 WT mice (n=5) receiving a mPTCL. Data are representative of 14 independent experiments using different mPTCLs. **(D)** Distribution of CD4 and CD8 receptor expression among mPTCLs (n=80). In the legend, DN means double CD4- and CD8-negative. **(E)** Scatter plot representation of surface expression of TCRβ, TCRγδ, CD5, CD25, CD127, PD1 and LAG3 measured by flow cytometry in mPTCLs (n=23) compared with normal total T cells (n=5) or gated on normal γδ T cells (n=5). Scatter plot representation of CD1d tetramer binding measured by flow cytometry on mPTCLs (n=10) compared with normal NKT cells from liver (n=3). P-values were determined by Mann-Whitney tests between mPTCLs and the control T cell population. **(F)** Scatter plot representation of Fas/CD95 expression measured by flow cytometry in mPTCLs (n=8) compared to normal resting (n=3) and activated (n=3) T cells. P-value was determined by Kruskal-Wallis test between the different conditions.

Supplemental Figure 3: TCR and IL-15 is dispensable for mPTCL survival. **(A)** Kaplan-Meier survival curves of CD3εKO mice receiving an mPTCL and treated with isotype control (n=4) or agonist anti-CD3 (n=5). P-value was determined by Log-Rank test. Data are representative of two independent experiments using different mPTCLs. (**B**) Histogramms showing the expression of CD3ε or CD122 in a representative mPTCL genetically invalidated for *Cd3ε* (sgCD3, left panel) or for *Il2rb* (sgCD122, right panel) or transfected with control guides RNA control (sgCtrl). Data are representative of two independent experiment on different mPTCLs. **(C)** Kaplan-Meier survival curves of WT (n=4) and *IL-15*$^{-/-}$ (n=4) mPTCL-

recipient mice. P-value was determined by Log-Rank test. Data are representative of three independent experiments. **(D)** Kaplan-Meier survival curves of mPTCL-recipient WT mice treated with anti-CD122 blocking mAb (n=5) or isotype control (n=5). P-value was determined by Log-Rank test. Data are representative of three independent experiments. **(E)** Kaplan-Meier survival curves of WT mice (n=5 per group) receiving mPTCL and treated with ruxolitinib (60 mg/kg), tofacitinib (10 mg/kg) or vehicle alone. P-values were determined by Log-Rank test. Data are representative of two independent experiments using different mPTCLs.

Supplemental Figure 4: NK-like reprogramming of mPTCL; (A) Heatmap of the top 140 genes most differentially expressed between mPTCLs and normal T cells (either stimulated or not). **(B)** Immunoblots showing Bcl11b protein expression in normal T cells and in 7 different mPTCLs. GAPDH expression was used as a loading control. **(C)**. PCA representation of mPTCLs, immature and mature T cells populations as well as mature NK cells, from ImmGen and from our own cohort based on the normalized accessibility of all 98,375 OCRs identified in ATAC-seq. (**D**) PCA representation of normal T cells, NK cells and mPTCLs based on the 310 significantly different methylated gene features between NK and T cells identified in RRBS (FDR < 0.01). (**E**) Boxplots calculated for each sample from the average methylation across ATAC-seq peaks with positive fold-change (FRD<0.01, logFc>0, n=144, left panel) and those with a negative fold-change (FDR<0.01, logFC<0, n=239, right panel). **(F)** Representative histograms of Eomes and T-bet expression determined by flow cytometry. Scatter plots of Eomes and T-bet expression in mPTCLs (n=23) compared to T (n=5) and NK cells (n=5). P-values were determined by Mann-Whitney tests between mPTCLs and normal T cells.

Supplemental Figure 5: NKR expression on murine and human PTCLs. (A) Distribution of activating (red), inhibitory (blue) and whole NKR (black) expression in mPTCLs (n=23). **(B)** Scatter plot representation of the percentage of positive lymphoma cells (three left graphs) or Delta MFI (three right graphs) of NKR measured by flow cytometry in mPTCL (n=26) compared to normal T and NK cells (n=3). P-values were determined by Mann-Whitney tests between mPTCLs sand control T cells. **(C)** CD28 expression measured by FACS analysis in mPTCL subgroups according to their expression of KLRG1 or NKG2D. P-values were determined by Mann-Whitney tests between the two subsets. **(D)** Heatmap representation of NK cell-associated gene expression in different human PTCL entities. Genes in the heatmap are shown in rows, and each individual sample is shown in one column. The scale bar shows color-coded differential expression from the mean in SD units, with yellow indicating higher expression and blue indicating lower expression. **(E)** Heatmap showing the expression of NK cell signature using genes defined in (D) in human PTCL-NOS molecular TBX21, GATA3 and

unclassified subgroups. **(F)** GSEA analysis of NK cell gene signature. Upward deflection of the green line indicates that PTCL-TBX21 are significantly enriched for genes associated with the NK signature, compared to PTCL-GATA3 (p=0.04, FDR=0.09). **(G)** Overall survival (OS) in PTCL-TBX21 subgroups according to the NK-cell signature. Prognostic subgroups were defined according to the mean expression of NK-cell gene signature, when dividing the PTCL-TBX21 into three equal groups (tertiles) as color-coded in (A). **(H)** Scatter plot representation of FACS analysis of NKR expression in 9 different entities of human PTCLs and normal NK cells. **(I)** Distribution of KIR3DL2, KIRs, NKG2s and NCRs expression in the whole human PTCL cohort.

Supplemental Figure 6: *In vivo* blockade of NKR signaling prolonged mouse survival. (A) Histogramms showing the expression of NKG2D or NKp46 in mPTCL cells genetically invalidated for *Klrk1* (sgNKG2D), *Ncr1* (sgNKp46) or both, using Alt-R® CRISPR-Cas9 guide RNA targeting these genes or transfected with control guide RNA (sgCtrl). Data are representative of two independent experiment on different mPTCLs. MFIs of NKG2D or NKp46 stainings for each condition are indicated**. (B)** Weights of spleen (left panel) and liver (right panel) of mPTCL-recipient NSG mice treated with anti-NKp46 and anti-NKG2D blocking mAbs (n=5) or isotype control (n=5) and euthanized 12 days post PTCL transfer. **(C)** Spleen (left panel) and liver (right panel) cell counts in mPTCL-recipient NSG mice treated with anti-NKp46 and anti-NKG2D blocking mAbs (n=5) or isotype control (n=5) and euthanized 12 days post mPTCL transfer. (**D**) Western blot showing the expression of Syk and GAPDH in mPTCL cells genetically invalidated for *Syk* (sgSyk) or transfected with control guide RNA (sgCtrl). Data are representative of two independent experiment on different mPTCLs. **(E)** FACS analysis of Pan-Rae1 expression by different cell types in spleens (n=8). **(F)** Scatter plots of Pan-Rae1 expression by different cell types in spleens measured by flow cytometry.

Supplemental Table 1 : mPTCL characterization by IHC compared with flow cytometry.

	Organ	Lymphoma invasion by FCM[a] (%)	Lymphoma invasion by IHC[b] (%)	HPS interpretation	CD3 staining by FCM	CD3 staining by IHC
PTCL#1	Liver	85	30	Effacement of the liver architecture with perivascular and intrasinusoidal tumoral cell infiltration	positive	low
	Spleen	60	nd	Diffuse invasion of large cells	positive	low
	LN	70	nd	Invasion of large cells with sign of aggressiveness	positive	low
PTCL#2	Liver	70	70	Effacement of the liver architecture with massive infiltration of large cells	positive	low
	Spleen	60	80	Diffuse invasion of large cells	positive	low
PTCL#3	Liver	80	60	Effacement of the liver architecture with perivascular and nodal tumoral cell infiltration	negative	negative
	Spleen	35	20	Diffuse invasion of large cells	negative	negative
PTCL#4	Liver	45	30	Effacement of the liver architecture with intrasinusoidal and nodal tumoral cell infiltration	positive	low
	Spleen	60	70	Diffuse invasion of large cells	positive	low
PTCL#5	Liver	70	60	Complete effacement of the liver architecture with massive perivascular and intrasinusoidal tumoral cell infiltration	negative	negative
	Spleen	85	90	Massive invasion of large cells	negative	negative
	LN	75	80	Invasion of large cells	negative	negative
PTCL#6	Liver	95	70	Complete effacement of the liver architecture with massive perivascular and intrasinusoidal tumoral cell infiltration	positive	positive
	Spleen	55	60	Diffuse invasion of large cells	positive	positive
	LN	30	50	Invasion of large cells	positive	positive

[a]. FCM means flow cytometry.
[b]. IHC means immunohistochemistry.

Supplemental Table 2: clonality and phenotypic characteristics of mPTCLs

PTCL	% Clone[a]	V rearrangement[b]	D rearrangement[b]	J rearrangement[b]	sCD3[c]	co-receptor[c]
1	99.69	TCRBV01-01*01	UNKNOWN	TCRBJ02-04*01	+	CD4
2	99.55	TCRBV14-01*01	TCRBD02-01*01	TCRBJ02-05*01	+	CD8
3	99.84	TCRBV29-01*01	TCRBD01-01*01	TCRBJ01-03*01	+	CD4
4	94.17	TCRBV20-01*01	TCRBD01-01*01	TCRBJ01-03*01	+	CD8
5	98.52	TCRBV03-01*01	TCRBD02-01*01	TCRBJ02-03*01	++	CD8
6	93.97	TCRBV20-01*01	TCRBD01-01*01	TCRBJ01-03*01	+++	CD8
7	93.48	TCRBV12-02*01	TCRBD02-01*01	TCRBJ02-01*01	+	CD8
8	98.67	TCRBV01-01*01	UNKNOWN	TCRBJ01-06*01	+	DN
9	68.60	TCRBV13-03*01	UNKNOWN	TCRBJ02-03*01	+	DN
10	84.20	TCRBV19-01*01	UNKNOWN	TCRBJ01-01*01	++	CD8
11	83.28	TCRBV19-01*01	TCRBD02-01*01	TCRBJ01-04*01	++	CD8
12	75.06	TCRBV31-01*01	TCRBD01-01*01	TCRBJ01-03*01	+	CD8
13	98.91	TCRBV17-01*01	TCRBD02-01*01	TCRBJ02-01*01	+	CD8
14	99.23	TCRBV29-01*01	TCRBD01-01*01	TCRBJ01-04*01	+	DN
15	98.15	TCRBV20-01*01	TCRBD01-01*01	TCRBJ02-04*01	++	CD8
16	90.70	TCRBV26-01*01	TCRBD01-01*01	TCRBJ01-06*01	-	DN

[a]Clone productive frequencies of the TCRß chain rearrangement were determined after sequencing using the ImmunoSEQ kit.

[b]TCRBV, TCRBD and TCRBJ rearrangements were determined using ImmunoSEQ kit.

[c] Surface CD3 (sCD3), CD4 and CD8 expression were assessed by flow cytometry.

Supplemental Table 3 : Lymphoma cell phenotype for each patient

Entity	Age	Tissue	CD3	CD4	CD8	CD5	CD7	CD10	CD30	TiA1	GrzB	PD1	CXCL13	Bcl6	ICOS	SYK	PLCG2
ALCL ALK neg	30	Bone	neg	neg	neg	*nd*	*nd*	*nd*	pos	*nd*	*nd*	*nd*	*nd*	*nd*	*nd*	pos	pos
ALCL ALK neg	73	LN	neg	neg	neg	*nd*	*nd*	*nd*	pos	*nd*	*nd*	*nd*	*nd*	*nd*	*nd*	neg	neg
ALCL ALK neg	55	mesenteriq	pos	neg	neg	neg	pos	*nd*	pos	neg	pos	*nd*	*nd*	*nd*	*nd*	neg	pos
ALCL ALK neg	*nd*	LN	pos	pos	neg	neg	neg	neg	pos	neg	*nd*	*nd*	*nd*	*nd*	*nd*	neg	neg
ALCL ALK neg	82	LN	neg	*nd*	*nd*	*nd*	*nd*	*nd*	pos	neg	*nd*	*nd*	*nd*	*nd*	*nd*	neg	low
ALCL ALK neg	48	LN	neg	pos	neg	*nd*	*nd*	neg	pos	neg	neg	*nd*	*nd*	*nd*	*nd*	neg	pos
ALCL ALK neg	77	LN	neg	pos	neg	pos	pos	*nd*	pos	neg	pos	*nd*	*nd*	*nd*	*nd*	neg	neg
ALCL ALK neg	61	Unknown	pos	pos	*nd*	pos	pos	*nd*	pos	neg	neg	*nd*	*nd*	*nd*	*nd*	neg	neg
ALCL ALK neg	56	LN	pos	pos	*nd*	*nd*	*nd*	*nd*	pos	*nd*	neg	*nd*	*nd*	*nd*	*nd*	low	pos
ALCL ALK neg	48	LN	pos	pos	neg	pos	*nd*	neg	pos	neg	neg	*nd*	*nd*	*nd*	*nd*	neg	pos
ALCL ALK neg	50	Cavum	pos	pos	neg	*nd*	pos	*nd*	pos	pos	pos	*nd*	*nd*	pos	*nd*	neg	pos
ALCL ALK neg	47	LN	neg	neg	neg	neg	neg	*nd*	pos	*nd*	pos	*nd*	*nd*	*nd*	*nd*	neg	neg
ALCL ALK neg	85	LN	*nd*	*nd*	*nd*	*nd*	*nd*	*nd*	*nd*	*nd*	*nd*	*nd*	*nd*	*nd*	*nd*	neg	neg
ALCL ALK neg	16	LN	*nd*	*nd*	*nd*	*nd*	*nd*	*nd*	*nd*	*nd*	*nd*	*nd*	*nd*	*nd*	*nd*	low	pos
ALCL ALK neg	11	LN	*nd*	*nd*	*nd*	*nd*	*nd*	*nd*	*nd*	*nd*	*nd*	*nd*	*nd*	*nd*	*nd*	neg	pos
ALCL ALK neg	58	LN	*nd*	*nd*	*nd*	*nd*	*nd*	*nd*	*nd*	*nd*	*nd*	*nd*	*nd*	*nd*	*nd*	neg	neg
ALCL ALK neg	11	LN	*nd*	*nd*	*nd*	*nd*	*nd*	*nd*	*nd*	*nd*	*nd*	*nd*	*nd*	*nd*	*nd*	neg	pos
ALCL ALK pos	20	LN	neg	pos	neg	neg	*nd*	*nd*	pos	low	neg	*nd*	*nd*	*nd*	*nd*	neg	neg
ALCL ALK pos	55	LN	neg	pos	neg	*nd*	*nd*	*nd*	pos	*nd*	pos	*nd*	*nd*	*nd*	*nd*	pos	pos
ALCL ALK pos	19	LN	neg	low	neg	low	*nd*	*nd*	pos	pos	pos	*nd*	*nd*	*nd*	*nd*	neg	neg
ALCL ALK pos	72	LN	neg	pos	*nd*	neg	neg	*nd*	pos	pos	*nd*	*nd*	*nd*	*nd*	*nd*	low	pos
ALCL ALK pos	23	LN	*nd*	*nd*	*nd*	*nd*	*nd*	*nd*	*nd*	*nd*	*nd*	*nd*	*nd*	*nd*	*nd*	neg	neg
ALCL ALK pos	68	LN	*nd*	*nd*	*nd*	*nd*	*nd*	*nd*	*nd*	*nd*	*nd*	*nd*	*nd*	*nd*	*nd*	pos	low
ALCL ALK pos	*nd*	*nd*	*nd*	*nd*	*nd*	*nd*	*nd*	*nd*	*nd*	*nd*	*nd*	*nd*	*nd*	*nd*	*nd*	neg	pos
ALCL ALK pos	17	LN	*nd*	*nd*	*nd*	*nd*	*nd*	*nd*	*nd*	*nd*	*nd*	*nd*	*nd*	*nd*	*nd*	pos	pos
ALCL ALK pos	19	LN	*nd*	*nd*	*nd*	*nd*	*nd*	*nd*	*nd*	*nd*	*nd*	*nd*	*nd*	*nd*	*nd*	pos	pos
ALCL ALK pos	61	LN	*nd*	*nd*	*nd*	*nd*	*nd*	*nd*	*nd*	*nd*	*nd*	*nd*	*nd*	*nd*	*nd*	neg	pos
ALCL ALK pos	9	Skin	*nd*	*nd*	*nd*	*nd*	*nd*	*nd*	*nd*	*nd*	*nd*	*nd*	*nd*	*nd*	*nd*	pos	neg
ALCL ALK pos	40	LN	*nd*	*nd*	*nd*	*nd*	*nd*	*nd*	*nd*	*nd*	*nd*	*nd*	*nd*	*nd*	*nd*	neg	neg
ALCL ALK pos	40	LN	*nd*	*nd*	*nd*	*nd*	*nd*	*nd*	*nd*	*nd*	*nd*	*nd*	*nd*	*nd*	*nd*	neg	pos
ALCL ALK pos	11	LN	*nd*	*nd*	*nd*	*nd*	*nd*	*nd*	*nd*	*nd*	*nd*	*nd*	*nd*	*nd*	*nd*	pos	pos
ALCL ALK pos	39	LN	*nd*	*nd*	*nd*	*nd*	*nd*	*nd*	*nd*	*nd*	*nd*	*nd*	*nd*	*nd*	*nd*	neg	neg
ALCL ALK pos	16	LN	low	*nd*	*nd*	*nd*	*nd*	*nd*	pos	*nd*	neg	*nd*	*nd*	*nd*	*nd*	pos	pos
ALCL ALK pos	15	LN	neg	neg	neg	neg	*nd*	*nd*	pos	*nd*	pos	*nd*	*nd*	*nd*	*nd*	pos	neg
ALCL ALK pos	35	LN	neg	pos	*nd*	pos	*nd*	*nd*	pos	*nd*	*nd*	*nd*	*nd*	*nd*	*nd*	neg	pos
TFH-like	83	LN	pos	pos	neg	pos	neg	pos	*nd*	neg	*nd*	*nd*	*nd*	*nd*	*pos*	neg	neg
TFH-like	59	LN	pos	pos	neg	*nd*	*nd*	pos	*nd*	*nd*	*nd*	*nd*	*nd*	*nd*	*nd*	pos	pos
TFH-like	53	LN	pos	pos	neg	*nd*	*nd*	pos	neg	*nd*	*nd*	*nd*	*nd*	pos	*nd*	neg	neg
TFH-like	70	LN	pos	pos	neg	*nd*	*nd*	pos	low	*nd*	*nd*	pos	pos	pos	*nd*	pos	neg
TFH-like	86	LN	pos	pos	neg	*nd*	*nd*	*nd*	neg	*nd*	*nd*	pos	pos	*nd*	*nd*	neg	neg
TFH-like	78	LN	pos	pos	neg	pos	*nd*	neg	neg	*nd*	*nd*	pos	*nd*	pos	*nd*	pos	pos
TFH-like	87	LN	pos	pos	neg	pos	pos	neg	neg	*nd*	*nd*	pos	pos	*nd*	*nd*	pos	neg
TFH-like	74	LN	pos	pos	neg	*nd*	*nd*	low	low	*nd*	*nd*	pos	pos	*nd*	*nd*	neg	neg
TFH-like	86	LN	pos	pos	neg	*nd*	*nd*	neg	low	*nd*	*nd*	pos	low	neg	*nd*	pos	neg
TFH-like	75	LN	pos	pos	neg	pos	neg	neg	pos	*nd*	neg	pos	neg	pos	*nd*	neg	neg
TFH-like	76	LN	pos	pos	neg	*nd*	pos	neg	neg	*nd*	*nd*	pos	low	neg	*nd*	neg	neg
TFH-like	81	LN	pos	pos	neg	*nd*	neg	pos	low	*nd*	neg	pos	pos	*nd*	*nd*	pos	neg
TFH-like	54	LN	pos	pos	neg	*nd*	pos	*nd*	*nd*	*nd*	*nd*	pos	pos	*nd*	*nd*	neg	neg

TFH-like	70	LN	pos	pos	neg	pos	pos	pos	*nd*	*nd*	*nd*	pos	pos	pos	*nd*	pos	pos
TFH-like	53	LN	pos	pos	neg	pos	neg	pos	neg	*nd*	*nd*	pos	pos	pos	*nd*	neg	neg
TFH-like	30	LN	pos	pos	neg	pos	pos	pos	neg	*nd*	*nd*	pos	pos	pos	*nd*	pos	pos
TFH-like	66	LN	pos	pos	neg	pos	low	low	neg	low	neg	pos	low	pos	*nd*	neg	neg
TFH-like	76	LN	pos	pos	neg	*nd*	*nd*	pos	neg	*nd*	*nd*	pos	pos	pos	*nd*	pos	neg
TFH-like	67	LN	pos	pos	neg	pos	*nd*	pos	pos	*nd*	*nd*	pos	pos	pos	*nd*	pos	neg
TFH-like	35	LN	pos	pos	neg	low	low	neg	neg	neg	neg	pos	pos	pos	*nd*	neg	neg
TFH-like	53	LN	pos	*nd*	*nd*	pos	*nd*	low	*nd*	*nd*	*nd*	pos	low	neg	*nd*	pos	pos
TFH-like	57	LN	pos	*nd*	*nd*	*nd*	*nd*	neg	*nd*	*nd*	*nd*	low	low	*nd*	*nd*	neg	neg
TFH-like	69	LN	pos	pos	neg	pos	pos	low	*nd*	*nd*	*nd*	pos	pos	low	*nd*	neg	neg
TFH-like	35	LN	pos	*nd*	*nd*	pos	*nd*	pos	*nd*	*nd*	*nd*	pos	low	pos	*nd*	neg	neg
TFH-like	75	LN	pos	pos	*nd*	pos	*nd*	low	*nd*	*nd*	*nd*	low	low	low	*nd*	neg	neg
TFH-like	*nd*	LN	pos	pos	neg	pos	low	neg	*nd*	*nd*	*nd*	pos	pos	low	*nd*	neg	neg
TFH-like	*nd*	LN	pos	pos	*nd*	pos	pos	low	*nd*	*nd*	*nd*	pos	pos	pos	*nd*	low	low
TFH-like	45	LN	pos	pos	*nd*	pos	low	pos	*nd*	*nd*	*nd*	pos	*nd*	low	*nd*	low	neg
TFH-like	53	LN	pos	pos	neg	*nd*	*nd*	pos	*nd*	*nd*	*nd*	pos	pos	pos	*nd*	pos	pos
TFH-like	67	LN	pos	*nd*	*nd*	pos	*nd*	pos	*nd*	*nd*	*nd*	pos	low	low	*nd*	neg	neg
TFH-like	80	LN	pos	pos	neg	pos	neg	low	*nd*	*nd*	*nd*	pos	*nd*	low	*nd*	neg	neg
TFH-like	75	LN	pos	pos	neg	pos	low	low	*nd*	*nd*	*nd*	pos	low	low	*nd*	neg	neg
TFH-like	83	LN	pos	pos	neg	pos	low	pos	*nd*	*nd*	*nd*	pos	pos	*nd*	*nd*	neg	neg
TFH-like	87	LN	pos	pos	*nd*	pos	low	pos	*nd*	*nd*	*nd*	pos	pos	pos	*nd*	neg	neg
TFH-like	52	LN	pos	*nd*	*nd*	pos	*nd*	pos	low	*nd*	*nd*	pos	low	pos	*nd*	neg	neg
TFH-like	54	LN	pos	pos	neg	*nd*	*nd*	low	*nd*	*nd*	*nd*	pos	*nd*	*nd*	*nd*	neg	neg
TFH-like	64	LN	pos	*nd*	*nd*	pos	*nd*	pos	*nd*	*nd*	*nd*	pos	pos	*nd*	*nd*	low	neg
TFH-like	76	LN	pos	*nd*	*nd*	*nd*	*nd*	*nd*	*nd*	*nd*	*nd*	*nd*	*nd*	*nd*	*nd*	neg	neg
TFH-like	73	LN	pos	*nd*	*nd*	*nd*	*nd*	low	*nd*	*nd*	*nd*	low	*nd*	low	*nd*	neg	neg
TFH-like	51	LN	pos	*nd*	*nd*	*nd*	*nd*	low	*nd*	*nd*	*nd*	low	low	neg	*nd*	pos	low
TFH-like	76	LN	pos	pos	neg	*nd*	neg	low	*nd*	*nd*	*nd*	low	low	low	*nd*	neg	neg
TFH-like	79	LN	pos	*nd*	*nd*	pos	*nd*	pos	*nd*	*nd*	*nd*	pos	pos	pos	*nd*	neg	neg
TFH-like	63	LN	pos	pos	neg	pos	neg	pos	low	*nd*	*nd*	pos	pos	pos	*nd*	neg	neg
TFH-like	*nd*	LN	pos	*nd*	*nd*	pos	neg	pos	pos	*nd*	*nd*	pos	pos	pos	*nd*	neg	neg
TFH-like	71	LN	pos	pos	neg	pos	*nd*	low	*nd*	*nd*	*nd*	pos	*nd*	low	*nd*	neg	neg
TFH-like	57	LN	*nd*	pos	*nd*	pos	neg	*nd*	*nd*	*nd*	*nd*	pos	*nd*	low	*nd*	neg	neg
TFH-like	*nd*	LN	pos	*nd*	*nd*	pos	neg	neg	*nd*	*nd*	*nd*	pos	neg	low	*nd*	neg	neg
TFH-like	66	LN	low	pos	neg	pos	pos	*nd*	*nd*	*nd*	*nd*	pos	pos	*nd*	*nd*	neg	neg
TFH-like	63	LN	pos	pos	*nd*	pos	*nd*	pos	*nd*	*nd*	*nd*	pos	pos	pos	*nd*	neg	neg
TFH-like	83	LN	pos	pos	*nd*	pos	pos	low	*nd*	*nd*	*nd*	pos	low	neg	*nd*	neg	neg
TFH-like	51	LN	pos	*nd*	*nd*	pos	neg	low	pos	*nd*	*nd*	pos	low	low	*nd*	neg	neg
TFH-like	*nd*	LN	pos	*nd*	*nd*	pos	pos	pos	low	*nd*	*nd*	*nd*	*nd*	*nd*	pos	neg	neg
TFH-like	62	LN	pos	pos	neg	pos	*nd*	pos	*nd*	*nd*	*nd*	pos	pos	pos	*nd*	neg	neg
TFH-like	73	LN	pos	pos	neg	pos	pos	low	pos	*nd*	*nd*	pos	low	pos	*nd*	neg	neg
TFH-like	57	Tegument	*nd*	*nd*	*nd*	*nd*	*nd*	*nd*	*nd*	*nd*	*nd*	*nd*	*nd*	*nd*	*nd*	neg	neg
TFH-like	61	LN	*nd*	*nd*	*nd*	*nd*	*nd*	*nd*	*nd*	*nd*	*nd*	*nd*	*nd*	*nd*	*nd*	neg	neg
TFH-like	85	Tongue	*nd*	*nd*	*nd*	*nd*	*nd*	low	*nd*	*nd*	*nd*	pos	pos	low	*nd*	pos	neg
TFH-like	53	LN	*nd*	*nd*	*nd*	*nd*	*nd*	*nd*	*nd*	*nd*	*nd*	*nd*	*nd*	*nd*	*nd*	neg	neg
TFH-like	62	Tonsil	*nd*	*nd*	*nd*	*nd*	*nd*	*nd*	*nd*	*nd*	*nd*	*nd*	*nd*	*nd*	*nd*	neg	neg
TFH-like	54	LN	pos	low	neg	*nd*	neg	neg	*nd*	neg	*nd*	pos	pos	pos	pos	neg	neg
HSTL	*nd*	Spleen	pos	neg	neg	neg	neg	*nd*	*nd*	pos	neg	*nd*	*nd*	*nd*	*nd*	neg	neg
HSTL	62	Spleen	pos	neg	neg	neg	*nd*	*nd*	*nd*	pos	neg	*nd*	*nd*	*nd*	*nd*	neg	neg
HSTL	*nd*	Spleen	pos	neg	neg	neg	*nd*	*nd*	*nd*	pos	neg	*nd*	*nd*	*nd*	*nd*	neg	neg
HSTL	35	Spleen	pos	neg	neg	neg	*nd*	*nd*	*nd*	pos	neg	*nd*	*nd*	*nd*	*nd*	neg	neg
HSTL	74	Spleen	pos	neg	neg	neg	*nd*	*nd*	neg	*nd*	*nd*	*nd*	*nd*	*nd*	*nd*	low	low
HSTL	42	Spleen	neg	neg	neg	neg	pos	*nd*	*nd*	*nd*	*nd*	*nd*	*nd*	*nd*	*nd*	low	low

HSTL	*nd*	Spleen	pos	neg	pos	neg	neg	*nd*	*nd*	pos	pos	*nd*	*nd*	*nd*	*nd*	neg	neg
HSTL	46	Spleen	pos	neg	neg	neg	pos	*nd*	*nd*	pos	neg	*nd*	*nd*	*nd*	*nd*	neg	neg
HSTL	*nd*	*nd*	*nd*	*nd*	*nd*	*nd*	*nd*	*nd*	*nd*	*nd*	*nd*	*nd*	*nd*	*nd*	*nd*	neg	neg
PTCL-NOS	61	LN	pos	neg	neg	*nd*	*nd*	*nd*	*nd*	pos	*nd*	*nd*	*nd*	*nd*	*nd*	neg	neg
PTCL-NOS	71	LN	pos	neg	pos	*nd*	*nd*	*nd*	pos	pos	*nd*	*nd*	*nd*	*nd*	*nd*	neg	neg
PTCL-NOS	61	Skin	pos	neg	neg	*nd*	*nd*	neg	*nd*	pos	pos	*nd*	*nd*	neg	*nd*	neg	neg
PTCL-NOS	67	LN	pos	low	neg	pos	*nd*	neg	neg	pos	low	*nd*	*nd*	neg	*nd*	neg	neg
PTCL-NOS	65	LN	pos	pos	neg	*nd*	neg	neg	neg	neg	neg	*nd*	*nd*	neg	*nd*	neg	neg
PTCL-NOS	65	LN	pos	pos	neg	pos	pos	neg	pos	neg	*nd*	*nd*	*nd*	neg	*nd*	neg	neg
PTCL-NOS	82	LN	neg	pos	neg	neg	*nd*	*nd*	pos	low	*nd*	*nd*	*nd*	*nd*	*nd*	neg	pos
PTCL-NOS	53	LN	neg	pos	neg	pos	low	neg	neg	neg	neg	neg	*nd*	neg	*nd*	neg	neg
PTCL-NOS	55	LN	pos	pos	neg	low	neg	neg	neg	neg	neg	neg	neg	neg	*nd*	pos	neg
PTCL-NOS	49	LN	pos	*nd*	*nd*	pos	pos	*nd*	neg	*nd*	*nd*	pos	neg	pos	*nd*	pos	neg
PTCL-NOS	72	Kidney	pos	pos	neg	pos	pos	neg	neg	neg	neg	pos	neg	neg	*nd*	neg	neg
PTCL-NOS	46	LN	pos	pos	neg	neg	neg	neg	pos	neg	neg	neg	*nd*	neg	*nd*	neg	neg
PTCL-NOS	70	LN	*nd*	*nd*	*nd*	*nd*	*nd*	*nd*	*nd*	*nd*	*nd*	*nd*	*nd*	*nd*	*nd*	neg	low
PTCL-NOS	82	Eye	pos	pos	neg	pos	neg	neg	*nd*	*nd*	*nd*	*nd*	*nd*	*nd*	*nd*	neg	neg
PTCL-NOS	74	LN	pos	pos	neg	pos	*nd*	neg	*nd*	*nd*	*nd*	neg	*nd*	pos	pos	neg	neg
PTCL-NOS	75	LN	pos	*nd*	*nd*	pos	*nd*	low	*nd*	*nd*	*nd*	pos	low	neg	pos	neg	neg
PTCL-NOS	46	Spleen	pos	*nd*	neg	*nd*	neg	neg	neg	pos	pos	*nd*	*nd*	*nd*	*nd*	neg	pos
PTCL-NOS	68	LN	pos	pos	neg	pos	*nd*	neg	neg	*nd*	neg	neg	neg	low	pos	neg	low
PTCL-NOS	67	LN	pos	pos	*nd*	pos	pos	*nd*	pos	*nd*	neg	*nd*	*nd*	*nd*	*nd*	neg	low
PTCL-NOS	52	LN	pos	pos	*nd*	pos	*nd*	low	low	*nd*	*nd*	*nd*	neg	*nd*	pos	neg	neg
PTCL-NOS	71	LN	pos	pos	neg	pos	*nd*	*nd*	pos	neg	*nd*	*nd*	*nd*	*nd*	*nd*	neg	neg
PTCL-NOS	69	LN	pos	pos	neg	pos	pos	*nd*	*nd*	*nd*	*nd*	*nd*	*nd*	*nd*	*nd*	neg	neg
PTCL-NOS	*nd*	LN	pos	neg	pos	neg	*nd*	low	low	*nd*	*nd*	low	low	pos	neg	neg	neg
PTCL-NOS	61	LN	pos	pos	neg	pos	*nd*	neg	pos	*nd*	*nd*	*nd*	neg	pos	pos	neg	low
PTCL-NOS	64	LN	pos	pos	neg	pos	neg	neg	*nd*	neg	neg	*nd*	*nd*	neg	neg	neg	neg
PTCL-NOS	64	LN	*nd*	*nd*	*nd*	*nd*	*nd*	*nd*	*nd*	*nd*	*nd*	*nd*	*nd*	*nd*	*nd*	neg	neg
PTCL-NOS	45	LN	pos	pos	low	pos	*nd*	neg	pos	pos	*nd*	neg	low	pos	*nd*	neg	neg
PTCL-NOS	66	Tonsil	pos	pos	*nd*	pos	*nd*	*nd*	pos	*nd*	neg	*nd*	*nd*	*nd*	*nd*	neg	neg
PTCL-NOS	67	Spleen	*nd*	*nd*	*nd*	*nd*	*nd*	*nd*	*nd*	*nd*	*nd*	*nd*	*nd*	*nd*	*nd*	neg	neg
PTCL-NOS	58	LN	pos	*nd*	*nd*	low	low	neg	pos	low	*nd*	neg	*nd*	low	*nd*	neg	low
PTCL-NOS	44	LN	pos	pos	neg	pos	pos	neg	neg	neg	neg	pos	neg	neg	pos	neg	neg
PTCL-NOS	58	LN	*nd*	*nd*	*nd*	*nd*	*nd*	*nd*	*nd*	*nd*	*nd*	*nd*	*nd*	*nd*	*nd*	neg	low
MEITL	32	Digestive	pos	neg	pos	neg	*nd*	*nd*	*nd*	pos	pos	*nd*	*nd*	*nd*	*nd*	neg	neg
MEITL	73	Duodenum	pos	neg	pos	neg	pos	neg	neg	*nd*	pos	*nd*	*nd*	*nd*	*nd*	neg	neg
MEITL	*nd*	Prostate	pos	neg	neg	*nd*	pos	pos	neg	pos	low	*nd*	*nd*	*nd*	*nd*	neg	neg
MEITL	85	Small intestine	pos	neg	pos	neg	pos	*nd*	*nd*	pos	pos	*nd*	*nd*	*nd*	*nd*	pos	neg
MEITL	73	Small intestine	pos	neg	pos	neg	pos	*nd*	*nd*	pos	low	*nd*	*nd*	*nd*	*nd*	pos	pos
MEITL	51	Small intestine	pos	neg	low	neg	pos	*nd*	*nd*	pos	low	*nd*	*nd*	*nd*	*nd*	pos	neg
MEITL	64	Small intestine	pos	neg	pos	neg	pos	*nd*	*nd*	pos	low	*nd*	*nd*	*nd*	*nd*	pos	pos
MEITL	81	Small intestine	pos	neg	pos	neg	pos	*nd*	*nd*	pos	low	*nd*	*nd*	*nd*	*nd*	low	neg
MEITL	74	Ileon	pos	neg	pos	neg	pos	*nd*	*nd*	low	neg	*nd*	*nd*	*nd*	*nd*	neg	neg
MEITL	45	Small intestine	pos	neg	low	neg	pos	*nd*	*nd*	pos	pos	*nd*	*nd*	*nd*	*nd*	pos	neg
MEITL	79	Small intestine	low	neg	pos	neg	low	*nd*	*nd*	pos	pos	*nd*	*nd*	*nd*	*nd*	neg	neg
MEITL	80	Small intestine	pos	neg	pos	neg	pos	*nd*	*nd*	pos	pos	*nd*	*nd*	*nd*	*nd*	low	neg
MEITL	67	Small intestine	pos	neg	pos	neg	pos	*nd*	*nd*	pos	low	*nd*	*nd*	*nd*	*nd*	neg	neg
MEITL	77	Small intestine	pos	neg	low	neg	pos	*nd*	*nd*	pos	pos	*nd*	*nd*	*nd*	*nd*	pos	neg
MEITL	64	Small intestine	low	low	low	neg	pos	*nd*	*nd*	pos	pos	*nd*	*nd*	*nd*	*nd*	low	neg
EATL	61	LN	low	pos	neg	*nd*	pos	neg	pos	neg	*nd*	*nd*	*nd*	*nd*	low	neg	low
EATL	55	LN	pos	*nd*	pos	*nd*	*nd*	*nd*	low	pos	pos	*nd*	*nd*	*nd*	*nd*	neg	neg
EATL	66	LN	pos	*nd*	neg	neg	*nd*	*nd*	neg	neg	neg	*nd*	*nd*	*nd*	*nd*	neg	neg

EATL	63	Small intestine	pos	neg	pos	*nd*	*nd*	*nd*	neg	pos	pos	*nd*	*nd*	*nd*	*nd*	neg	neg
EATL	86	Small intestine	pos	neg	pos	neg	*nd*	neg	neg	pos	neg	*nd*	*nd*	*nd*	*nd*	neg	low
EATL	67	Duodenum	pos	*nd*	neg	neg	*nd*	*nd*	pos	pos	pos	*nd*	*nd*	*nd*	*nd*	neg	neg

Supplemental Table 4 : Gene list of the three clusters defined in Figure 4B.

Gene list Cluster 1					
Abcb1a	Cd44	**Fasl**	Itgae	Nr4a1	**Tbx21**
Ahnak	Cd7	Gsap	Itgax	Nrp1	Tcrg-C4
Anxa1	Chn2	**Gzmb**	Jun	Osbpl3	Tcrg-V4
Atp8b4	Cpa3	**Id2**	**Klrb1c**	Pdcd1	Trat1
AW112010	Cst7	Ikzf2	**Klrc1**	Pglyrp1	Ttc39b
Bhlhe40	Ctla2a	Il12rb2	**Klrc3**	Plac8	Ttc39c
Casp1	Ctse	Il17rb	**Klrd1**	Plek	
Ccl3	Ctsw	Il18r1	**Klrk1**	Ptprj	
Ccl5	Dusp1	Il18rap	Ly6a	Rgs1	
Ccr2	Entpd1	Il2ra	Myo1f	S100a6	
Ccr5	Fam129a	Itga1	**Nkg7**	Slamf7	
Gene list Cluster 2					
Anln	Ccnb2	E2f8	Kif2c	Nt5dc2	Rrm2
Anxa2	Cd24a	Ect2	Kif4	Nuf2	Shcbp1
Arpp21	Cdca7	Fads2	Kit	Nusap1	Ska3
Bub1	Cenpe	Fignl1	Marcks	Plk1	Sox4
Bub1b	Cenph	Gzma	Marcksl1	Plxdc2	Stil
C330027C09Rik	Cep55	Hells	Myb	Prc1	Top2a
Ccna2	Chek1	Kif11	Ncapg	Prim1	Tpx2
Ccnb1	Dtl	Kif20a	Ncapg2	Qser1	Uhrf1
Gene list Cluster 3					
Art2b	Cd55	Eomes	Igfbp4	Ms4a4c	Slfn1
Ccr4	**Cd8a**	Ephx1	Il2rb	Nsg2	Slfn5
Ccr7	**Cd8b1**	Gimap3	Il6ra	Nt5e	Snord22
Ccr8	Crtam	Gimap4	Il6st	P2rx7	St6gal1
Ccr9	Cxcr3	Gimap7	**Il7r**	Pde2a	St8sia1
Cd2	Cxcr6	Gramd3	Inpp4b	S1pr1	Tdrp
Cd226	Dapl1	**Icos**	Itgb3	Samhd1	Tnfsf8
Cd4	Dntt	Ifngr2	Itm2a	**Sell**	Zbtb7b
Cd40lg	Dtx1	Ift80	Ms4a4b	Sidt1	

Supplemental Table 5: Sequence of guide RNA targeting *Syk, Cd3e, Il2rb, Ncr1, Klrk1*.

Name	Strand	Sequence
Mm.Cas9.SYK.1.AA	-	GCCATTAAGTTCCCTCTCGA
Mm.Cas9.SYK.1.AB	+	CCGGGAGTACAGCCCAAGAC
Mm.Cas9.SYK.1.AC	+	ATTGCACTACCGCATTGACA
Mm.Cas9.CD3E.1.AA	+	AGGGCACGTCAACTCTACAC
Mm.Cas9.CD3E.1.AB	-	TGATAAGCACCTGGTGCTCC
Mm.Cas9.CD3E.1.AC	-	ATGCGGTGGAACACTTTCTG
Mm.Cas9.IL2RB.1.AA	+	GGTTCGACTTGGCATGGACG
Mm.Cas9.IL2RB.1.AB	+	GTGGCCCAGAAGACGTCTAC
Mm.Cas9.IL2RB.1.AC	+	TATGTCAAGGAGGTCCACGG
Mm.Cas9.NCR1.1.AA	+	GCTCTTACAACGACTATGCA
Mm.Cas9.NCR1.1.AB	+	ATGGAAACTCGGTGAACATC
Mm.Cas9.NCR1.1.AC	-	CTCTGTGAGCCCTAGTCACG
Mm.Cas9.KLRK1.1.AA	+	AGGACTCGAACAACGAACAT
Mm.Cas9.KLRK1.1.AB	-	GCACTAACTACCAGTCAACC
Mm.Cas9.KLRK1.1.AC	-	CGACCTCAAGCCAGCAAAGT

SUPPLEMENTAL METHODS

Mice

p53$^{-/-}$ *(B6.129S2*-Trp53^{tm1Tyj}/J, RRID:MGI:3616345) and *IL-15*$^{-/-}$ (B6-Il15tm1Imx, RRID:MGI:3590155) mice were purchased from The Jackson Laboratory. *CD3ε*$^{-/-}$ (C57BL/6-Cd3^{etm1Mal}, RRID:IMSR_EM:00047) mice were obtained from Dr M. Malissen (Centre d'Immunologie Marseille-Luminy, France). C57BL/6 WT (C57BL/6J, RRID: IMSR_JAX:000664), congenic C57BL/6J CD45.1 (B6.SJL-*Ptprc*^{a}*Pepc*^{b}/BoyCrl) and *NOD-SCID-GammaC* (*NSG*) (NOD-scid IL2Rγnull (NOD.Cg-Prkdcscid Il2rgtm1Wjl/SzJ, RRID:BCBC_4142) mice were purchased from Charles River. All mice were maintained in specific pathogen-free conditions at the Plateau de Biologie Expérimentale de la Souris (Ecole Normale Supérieure de Lyon, France). All studies and procedures were performed in accordance with EU guidelines and approved by the local Animal Ethics Evaluation Committee (CECCAPP).

Antibody staining and flow cytometry analysis

Murine experiments. Single-cell suspension prepared from normal spleen or enlarged organs (spleen, lymph nodes, liver) were stained with a panel of fluorescent-labeled antibodies in BD Horizon Brillant Stain Buffer (BD Biosciences, #563794). Viability staining was performed with fixable viability dyes efluor780 or efluor506 purchased from eBioscience. The following mAbs reactive with murine cells were purchased from BD Biosciences : B220 (RA3-6B2, Cat# 557669), CD4 (GK1.5, Cat# 743156), CD5 (53-7.3, Cat# RM550035), CD8 (53-6.7, Cat# 563332), CD19 (1D3, Cat# 551001), CD24 (MI/69, Cat# 553262), CD25 (PC61, Cat# 557192), CD30 (mCD30.1, Cat# 553825), CD44 (IM7, Cat# 559250), CD54 (3E2, Cat# 74), CD62L (MEL-14, Cat# 561917), CD122 (TM-β1, Cat# 740230), CD127 (A7R34, Cat# 566377), TCRß (H57-597, Cat# 553172), TCRγδ (GL3, Cat# 553177), KLRG1 (2F1, Cat# 561619), NK1.1 (PK136, Cat# 562921), Ly49-G2 (4D11, Cat# 742885), NKG2A (20d5, Cat# 740758), NKp46 (29.A1.4, Cat# 560757), phospho-Syk (I120-722, Cat# 560081), phospho-PLCg2 (K86-689.37, Cat# 558490), phospho-Akt (M89-61, Cat# 562599); Biolegend (BL): CD3 (145-2C11, Cat# 100348), Thy1.2 (30-H12, Cat# 105326), NKG2D (CX5, Cat# 130212), DNAM1 (10e5, Cat# 128803), Ly49A (YE1/48.10.6, Cat# 116810), 2B4 (m2B4(B6)458.1, Cat# 133503), PD-1 (RMP1-30, Cat# 109112), T-bet (4B10, Cat# 644832), CD115 (AFS98, Cat# 135529), Granzyme B (QA16A02, Cat# 372204); eBioscience : Eomes (Dan11mag, Cat# 12-4875-80); ThermoFischer: Tdt (19-3, Cat# 12-5846-82); Miltenyi biotec: Ly49D (4E5, Cat# 130-102-8), Pan-Rae1 (REA723, Cat# 130-111-283); Cell Signaling technologies : Phospho-S6 (Flow) (D57.2.2E, Cat# 14733; RRID). Anti-Ly49C (4LO3311) was a kind gift from T. Walzer. APC-

conjugated mouse CD1d-empty or -αGalCer (PBS57) tetramers were obtained from the NIH Tetramer Core Facility.

Intracellular detection of TdT, T-bet and EOMES was performed under standard conditions using the FOXP3 transcription factor permeabilization kit (eBiosciences) as recommended by the manufacturer's protocol.

For flow cytometry detection of phosphorylated intracellular proteins, cells were fixed with 2% paraformaldehyde (PFA, Electron Microscopy Sciences, # 15710) for 5 min at room temperature and permeabilized with 90% ice cold methanol on ice for 45 min and then incubated with phosphorylated motifs rabbit reactive antibodies for 30 min at 4°C.

Human experiments. Cell suspension were obtained from frozen lymphoma samples (spleen, lymph nodes, liver, blood). Cells were stained with a panel of fluorescent-labeled antibodies. Viability staining was performed with fixable viability dye Zombie UV (Cell Signaling Technology, #423107). The following mAbs reactive with human cells were purchased from BD Biosciences: CD3 (UCHT1, Cat# 557706), B220 (RA3-6B2, Cat# 55766), CD4 (RPAT4, Cat# 557695), CD5 (UCHT2), CD8 (SFCI21Thy2D3), CD7 (MT-701, Cat# 563650), CD30 (BerH8, Cat# 563500), DNAM1 (TX25), CD94 (HP-3D9, Cat# 562361), KIR2DS4 (179315, Cat# 564375); Biolegend: KIR2DL2 (DX27, Cat# 312604), KIR2DL1 (HP-MA4, Cat# 339505), NKp30 (P30-15, Cat# 325208), NKp46 (9E2, Cat# 331913); Miltenyi Biotec: KLRG1 (REA261, Cat# 130-103-638), NKG2A (REA110, Cat# 130-098-818); Beckman Coulter : KLRB1 (B30631, Cat# IM3450); R&D System: PanKIR2D (NKVFS1, Cat# 130-099-040); InnatePharma: KIR3DL2 (MOG1-13E4); and Thermofischer: CD57 (TB01, Cat# 48-0577-42).

All antibodies were used as direct conjugates to FITC/AF488, PE, PE-TexasRed/PE-Dazzle, PerCP-Cy5.5, PE-Cy7, BV421, BV605, BV711, BV785, BUV396, BUV496, BUV 796, APC, AF700 or APC-Cy7.

For all antibodies reactive with membrane antigens, corresponding isotype controls were purchased from the same suppliers. For phosphoflow analysis and other intracellular staining, staining was compared to Fluorescence Minus One (FMO). Delta Median Fluorescence Intensity (Delta-MFI) was calculated using the difference of MFI in staining and control conditions. For antigens with a bimodal expression on the cells of interest, data were measured in percentage of positive cells. Flow cytometry data were acquired using a LSR II cytometer (BD Biosciences) and analyzed using the FlowJo software (TreeStar).

Histopathology and immunohistochemistry

Mouse tissues were dissected and fixed in 10% buffered formalin and paraffin-embedded at the histopathology department of Centre Hospitalier Universitaire Lyon-Sud (CHLS, Lyon –

France). Tissue sections were subjected to hematoxylin and eosin staining using standard procedures. To perform Syk and PLCγ2 immunohistochemistry on murine and human PTCL samples, tissue sections were de-paraffinized followed by antigen-retrieval and endogenous peroxidase (HRP) activity blocking. The following mAbs reactive with murine or human cells were purchased from Cell Signalling Technologies: Syk (polyclonal, Cat # 2712, dilution 1:1000), PLCg2 (polyclonal, Cat# 3872, dilution 1:1000); Agilent: CD3 (A0452, Cat # A 0452), CD20 (L26, Cat # M 0755), CD30 (BerH2, Cat # M0751), CD68(KP1, Cat # M0814), Thermo Fisher: CD3 (SP7, Cat # MA1-90582). Species-specific biotinylated secondary antibodies in the presence of avidin–horseradish peroxidase were obtained from Jackson Immunoresearch: Anti-rat IgG (Cat # 312-005-003), anti-hamster IgG (Cat # 307-005-003), anti-mouse IgM Fab'(Cat # 115-006-07). Slides were revealed using DAB color substrate on a BenchMark-ULTRA/VENTANA (ROCHE, #07098740001).

After immunohistochemistry, tissue sections were counterstained with hematoxylin and SYK and PLCγ2 expression were analyzed on lymphoma cells. Slides were read, and photographed using a Nikon digital sight DS-Fi2 camera and NIS Elements software. Scoring (negative, low or positive) was applied, based on both the extent and intensity of the staining. No staining of tumor cells was considered negative; low staining corresponded to positivity in less than 50% of tumor cells and positive staining corresponded to positivity in more than 50%. Negative staining with no internal positive control were not interpreted. For staining intensity, undetectable staining was considered negative, low and positive staining were attributed to weak and moderate to strong intensities, respectively.

Editing with CRISPR/Cas9

mPTCL gene editing by CRISP/Cas9 RNP complexes was adapted from Seki et *al.* (1).

Precomplexing of Cas9/RNP. To prepare the duplex Alt-R crRNA and Alt-R tracr-RNA (IDT catalog number 1072534), oligos were mixed at equimolar concentrations and annealed by heating at 95°C for 5 min in PCR thermocycler and followed by slowly cooling to room temperature. In a PCR strip, three crRNA–tracrRNA duplexes and Alt-R S.p. HiFi Cas9 Nuclease V3 (IDT, Cat# 1081061) were gently mixed by pipetting up and down and incubated at room temperature for at least 10 min.

We used predesigned Alt-R CRISPR-Cas9 Negative Control crRNA (IDT, Cat# 1072544, 1072545, 1072546) for control guides and predesigned Alt-R® CRISPR-Cas9 guide RNA targeting Syk, Cd3ε, Il2rb, Ncr1, Klrk1 genes from IDT (Supplemental Table 5).

Nucleofection. Primary cell nucleofection solution, supplement solution (P4 Primary Cell 4D-Nucleofector X kit L V4XP-4024; Lonza) and Alt-R Cas9 Electroporation enhancer 100µM

(IDT, Cat# 1075916) were added to the Cas9-RNP complex. 10^7 mPTCL cells were resuspended in the nucleofection mix, transferred to nucleofection cuvette vessels (4D-Nucleofector X kit L; Lonza) and electroporated using a 4D nucleofector (4D-Nucleofector Core Unit: Lonza, AAF-1002B; 4D-Nucleofector X Unit: AAF-1002X; Lonza). Depending of mPTCLs, DS137 or CM137 program was selected. After nucleofection, prewarmed complete T cell media was used to transfer transfected cells into mice.

Adoptive transfers, PTCL development and organ process

Adoptive transfers. T cells from three to five 6- to 8-week-old *p53*$^{-/-}$ or C57BL/6J WT mice were pooled and isolated using a magnetic bead-based negative selection T-cell depletion kit (Miltenyi, # 130-095-130) followed by negative sorting on CD19 and CD24 to avoid B-cell and immature T-cell contamination. $5x10^5$ cells were transferred into 6- to 10-week-old immunocompromised CD3ε$^{-/-}$ recipient mice by retro-orbital injection. All groups of mice were age- and sex-matched. Proper T-cell transfers were verified by the analysis of T-cell presence in peripheral blood 3 weeks after injection. Mice were observed twice a week until PTCL symptoms appeared. Mice were sacrificed when tumors became clinically apparent and macroscopically infiltrated organs (liver, spleen and lymph nodes) were harvested.

Organ process and lymphoma cell isolation. Aside from analyses of intracellular signaling activation (Western blot, phosphoflow and kinome analyses), spleens and lymph nodes were digested at 37°C for 30 min using collagenase Ia (Sigma, # C9891), while livers were digested using collagenase IV (Worthington, # LS004189). Liver cells were washed in 1X PBS with 2% Hepes and 2% FBS, resuspended in 40% Percoll, deposited on a 80% Percoll Gradient (GE Healthcare, # 17-0891-01) and centrifuged to allow mononuclear cell isolation. Cell suspensions were lysed using ACK. Cells were then resuspended in complete medium, stained to identify lymphoma cells and either frozen to allow subsequent analysis or submitted to *in vitro* functional experiments.

To study intracellular signaling events occurring in PTCLs at basal state, infiltrated livers were processed using the GentleMACS device (Miltenyi Biotec) while maintaining cells at 4°C to avoid *ex vivo* phosphorylation modifications and samples were then processed as previously described. For Western blot and kinome experiments, lymphoma cells were then isolated using a negative enrichment selection anti-PE (Miltenyi, 130-048-801) after staining with anti-Gr1 (RB6-8C5), CD19 (1D3) and CD21 (7G6) mAb coupled with PE. Lymphoma cell purity was consistently > 96% (not shown).

Tumor transplantation and *in vivo* treatments

Tumor transplantation. Cell suspension containing $2x10^6$ cells isolated from lymphoma-infiltrated liver or spleen from diseased mice were transferred into immunocompetent syngeneic C57Bl/6J WT mice, immunocompromised *CD3ε*$^{-/-}$ or NSG mice using retro-orbital injection.

Mice were sex- and age-matched and randomly assigned to experimental or control groups after PTCL transfer. For survival analyses, mice were observed twice a week until the appearance of PTCL symptoms, and were sacrificed when tumors became clinically apparent in PTCL-recipient mice. For the tumor burden group, mice were all sacrificed 12 days post transfer in order to measure liver and spleen weight, and count infiltrating lymphoma cells.

In vivo pharmacological inhibition. P505-15 (Adooq, # A11952), cerdulatinib (Selleckchem, # S6734) and cyclosporin A (Sigma, # 3004) were dissolved in DMSO and diluted in a solution containing 0.5% Methylcellulose (ThermoFischer, # 9004-67-5), corn oil or 1X PBS, respectively, and daily administered orally for 21 consecutive days at a dose of 20 mg/kg. Rapamycin (Sigma, # 53123-88-9) was dissolved in DMSO and diluted in a solution of 30% polyethylene glycol (PEG, Sigma, # 202398) and 70% sterile H2O and daily administered intraperitoneally (i.p.) for 21 consecutive days following PTCL transfer at a dose of 25 mg/kg. Ruxolitinib (LC laboratories, #R-6688) was solubilized at 15 mg/ml in 1% DMSO, 0.5% hydroxypropylmethyl cellulose, 0.1% tween 80 and administered by oral gavage at 60 mg/kg twice a day for 15 consecutive days after PTCL transfer. Tofacitinib (Selleckchem, #SE-S5001) was solubilized at 2.5 mg/ml in 1% DMSO, 0.5% hydroxypropylmethyl cellulose, 0.1% tween 80 and daily administered by oral gavage at 10 mg/kg for 15 consecutive days after PTCL transfer.

TCR/CD3 in vivo complex activation. To test the effect of TCR/CD3 complex activation on PTCLs, we treated NSG PTCL-recipient mice with agonist anti-CD3 mAb (BioXcell, # BE0001-1) or isotype control. Antibodies were administered i.p. once a day, five days a week during two weeks from day one post PTCL transfer at a dose of 50 µg/injection.

NKR in vivo blockade. To test the effect of NKaR blockade on PTCL development, we treated NSG PTCL-recipient mice with either blocking antibodies or appropriate isotype control. Anti-NKG2D (BioXcell, HMG2D) and anti-NKp46 (Innate Pharma, 29A1.4, Fc silent) antibodies were diluted in 1X PBS and administered i.p. alone or in combination from day one post PTCL transfer onwards. Anti-NKG2D and anti-NKp46 and appropriate isotype controls were injected three times a week for two weeks at a dose of 200 µg/injection and once a week for two weeks at a dose of 50 µg/injection, respectively. For anti-NKG2D and anti-NKp46 treated and control groups, mice were randomly assigned to the survival cohort or to the tumor burden group.

To ascertain the functional impact of NKG2D and NKp46 blockade on key downstream signaling effectors, anti-NKG2D (200 µg/injection) and anti-NKp46 (50 µg/injection) or appropriate isotype controls were injected 24 h (i.p.) and 1 h (i.v.) prior to sacrificing mice, and organs were processed as previously described for phosphoflow analysis.

Micro-CT analysis. Tomodensitometry imaging of PTCL-recipient mice was performed at the Anican platform (CRCL, Lyon France) using a Quantum FX (Perkin Elmer) 2 h after caudal i.v. injection of contrast reagent (Exitron Nano, # 130-095-698). Images were reconstructed to allow liver and spleen 3D visualization. Organ volumes were calculated using the Analyze software (Caliper).

In vivo role of IL-15. To test the role of IL-15 on PTCL engraftment, PTCL cells were transferred in *IL-15*$^{-/-}$ or C57Bl/6J WT recipient mice. To rule out the effect of an autocrine secretion of IL-15 by PTCL cells, C57Bl/6J WT PTCL-recipient mice were treated with anti-CD122 (IL-2/15Rβ) blocking antibody (BioXcell, Tm-β1) or appropriate isotype control (BioXcell, LTF2). Antibodies were diluted in 1X PBS and administered i.p. three times a week for two weeks at a dose of 200 µg/injection from day five post PTCL transfer onwards.

***In vitro* experiments**

Cytotoxicity assays. To analyze the functionality of NKaR in murine PTCL, we stimulated NKaR-positive PTCLs with functional mAb reactive with NKG2D (clone A10, Thermofisher) (10 µg/ml), NK1.1 (BioXcell, clone PK136) (10 µg/ml) and anti-NKp46 (clone 29A1.4, kind gift from T. Walzer) (10 µg/ml) alone and in combination or CD3 (clone 145-2C11, ThermoFisher) and CD28 (Clone 37.51, Thermofisher) coated, as previously described. Cells were plated at 2x10^6/ml and cultured in RPMI with 10% FBS, 2% Hepes, 200 mM β-mercaptoethanol with monensin (BD, Cat# 554724) and anti-LAMP1 (BL, 1D4B) antibody for four hours in the presence of p505-15 (2µM) or DMSO. Cells were then harvested, stained for surface antigens and then permeabilized with cytofix-Cytoperm buffer (BD, Cat# 554723) and finally stained for interferon-γ (BL, XMG1.2).

NKaR in vitro stimulation. To study the effect of NKaR stimulation on PTCL cells, samples were enriched, as previously described and cultured at 10^7 cell/ml for 1 h in the presence of Syk inhibitor (2 µM), PI3K inhibitor (1 µM) or DMSO. Cells were then stimulated by adding soluble anti-NKG2D (clone A10, Thermofisher) (10 µg/ml), NK1.1 (clone PK136, Innate Pharma) (10 µg/ml) and anti-NKp46 (clone 29A1.4) (10 µg/ml) mAbs alone or in combination. Receptor engagement was then induced by primary mAb cross-linking with appropriate species-specific secondary antibodies at a concentration of 20 µg/ml (Jackson Immunoresearch, # 315-005-003, 312-005-003 and 307-005-003) for 2 min. Stimulation was stopped either with 4°C PBS 1X before cell lysis for WB experiments or by fixation using 2% paraformaldehyde

for 5 min at room temperature (PFA, Electron Microscopy Sciences, # 15710) before permeabilization with 90% ice cold methanol for protein phosphorylation analysis by flow cytometry.

Western blot (WB)

When not specified, WB analysis was performed on unstimulated and enriched PTCL cells after cell lysis (Roche, # 04693159001) with freshly added phosphatase inhibitor cocktails (Sigma, # p5726 & p0044). For immunoblot detection, we used the following antibodies: ZAP70 (99F2, Cat # 2705, dilution 1:1000), phospho-PLCg2 (polyclonal, Cat# 3871, dilution 1:1000), phospho-PLCg1 (D6M9S, Cat# 14008, dilution 1:1000), phospho-Akt (D9E, Cat# 4060, dilution 1:1000), phospho-ERK (dilution 1:1000), Syk (polyclonal, Cat # 2712, dilution 1:1000), PLCg2 (polyclonal, Cat# 3872, dilution 1:1000), PLCg1 (D9H10, Cat# 5690, dilution 1:1000), Akt (polyclonal, Cat# 9272, dilution 1:1000), ERK (dilution 1:1000), DAP12 (D7G1X, Cat # 12492, dilution 1:500), GAPDH (14C10, Cat # 2118, dilution 1:4,000), anti-rabbit-HRP (Cat # 7074, dilution 1:1000), anti-mouse-HRP (Cat # 7076, dilition 1:1000), anti-rat-HRP (Cat # 7077, dilition 1:1000) all purchased from Cell Signaling Technology. FcεRIγ (1:1000) antibodies were purchased from Merck-Millipore. Bcl11b (Cat # 650602, 1:1000) antibody was purchased from Biolegend. Specificity of Abs directed against total and phosphorylated SYK, ZAP70, PLCγ isoforms, was controlled using naïve sorted B and T cells (Purity >99%) stimulated for 2 min with either 20 µg/ml of anti-IgM (Jackson Immunoresearch) or 10 µg/ml of anti-CD3 crosslinked with 20 µg/ml of anti-rat (Jackson Immunoresearch).
Lysates were separated by SDS-PAGE and transferred to nitrocellulose membranes using the iBlot2 device (Life). When needed, membranes were stained for phospho-proteins, stripped and re-probed for total proteins. The blots were developed using Luminata reagent (Merck-Millipore, WBLUF0500) according to the manufacturer's instructions.

PamChip peptide microarrays for kinome analysis

For kinome analysis, tyrosine kinase PamChip® arrays were purchased from PamGene International BV (#32501). Each array contained 144 peptides as well as 4 control peptides. Sample incubation, detection and analysis were performed in a PamStation 12 according to the manufacturer's instructions. Briefly, extracts from enriched mPTCL cells or mature T cells were made using M-PER mammalian extraction buffer (Thermo Scientific, # 78501) containing 1:50 Halt phosphatase inhibitor cocktail (Thermo Scientific, # 78420) and 1:50 Halt protease inhibitor cocktail, EDTA-free (Thermo Scientific, # 78425) for 15 min on ice. The lysates were then centrifuged at 16,000 g for 15 min to remove all debris. The supernatant was aliquoted, snap-frozen in liquid nitrogen and stored at -80°C until further processing. Prior to incubation

with the kinase reaction mix, the arrays were blocked with 2% BSA in water for 30 cycles and washed 3 times with PK assay buffer. Kinase reactions were performed for 1 h with 5 µg of total extract and 4 µM ATP at 30°C. Phosphorylated peptides were detected with an anti-rabbit-FITC antibody that recognizes a pool of phospho-tyrosines. The instrument contains a 12-bit CCD camera suitable for imaging of FITC-labeled arrays. The images obtained from the phosphorylated arrays were quantified using the BioNavigator software (PamGene International BV), and the list of peptides of which the phosphorylation differed significantly between PTCLs and controls was uploaded to GeneGo for pathway analysis. The BioNavigator software was used to perform the upstream PTK analysis shown in Figure 3A.

Microarray analysis

Cell sorting. Lymphoma cells from thymus, spleen, lymph nodes or liver, were sorted on a FACSAria sorter (BD Biosciences). Purity was consistently >98% (not shown). Sorted normal T lymphocytes pooled from spleen and mesenteric lymph nodes from age-matched WT animal were used as controls. For normal T-cell activation, anti-CD3/anti-CD28 coated beads (Invitrogen, # 11453D) were used at a 1:1 bead-to-cell ratio in 3-day cultures.

Target labeling. Total RNA was extracted using TRIZOL Reagent (Invitrogen) and was amplified by *in vitro* transcription using an ExpressArt® C&E mRNA amplification nano kit (AmpTec GmbH, Hamburg, Germany). During this process, RNA was biotin-labeled using BioArray HighYield RNA Transcript Labeling Kit (Enzo Life Sciences, Inc., Farmingdale, New York, USA). Before amplification, spikes of synthetic mRNA (GeneChip® Eukaryotic Poly-A RNA Controls, Affymetrix, Santa Clara, CA, USA) at different concentrations were added to all samples; these positive controls were used to ascertain the quality of the process. Biotinylated antisense cRNA quantification was performed with a Nanodrop 1000 (Nanodrop, Wilmington, DE, USA) and quality checked with Agilent 2100 Bioanalyzer (Agilent technologies, Inc, Palto Alto, CA, USA).

Array hybridization, scanning and normalization. Hybridization was performed following the Affymetrix protocol. Briefly, 15 µg of labeled cRNA was fragmented and denaturated in hybridization buffer, 10 µg were then hybridized on GeneChip® Mouse Genome 430 2.0 array (Affymetrix) for 16 h at 45°C with constant mixing by rotation at 60 rpm in the Hybridization Oven 640 (Affymetrix). After hybridization, arrays were washed and stained with streptavidin-phycoerythrin (GeneChip® Hybridization Wash and Stain Kit) in the Fluidics Station 450 (Affymetrix) according to the manufacturer's instruction. The arrays were read with a confocal laser (GeneChip® Scanner 3000 7G, Affymetrix). The CEL files were generated with the Affymetrix GeneChip Command Console software 3.0. The data obtained were normalized

with the Affymetrix Expression Console software using MAS5 statistical algorithm. Gene Set Enrichment Analysis (GSEA) was performed using javaGSEA and R.

ATAC-Seq

10^4 sorted cells were washed with 1mL of pre-chilled PBS and cell pellets were suspended in 50 µL of reaction mixture: 25 µl of 2 × Tagmentation DNA buffer, 2.5 µl of Tn5 enzyme (Nextera DNA Library Preparation Kit, Illumina), 0.5 µl of 1% digitonin (#G9441, Promega) and 22 µl of nuclease-free water, as previously described (Corces et al., 2016). The reaction was incubated at 37 °C for 30 min with agitation at 300 rpm and transposed DNA was purified using a QIAgen MinElute Reaction Cleanup kit (QIAGEN, Courtaboeuf, France). ATAC-seq libraries were constructed by ligating Nextera sequencing primers (2) using PCR amplification. Briefly, a first round of PCR was assessed in a volume of 50 µL containing NEBNext High-Fidelity 2X PCR Master Mix (New England Biolabs, MA, USA) with primers (1.25 µM each) with the following thermal cycles: 72°C for 5 min, 98°C for 30 s, followed by 7 cycles [98°C for 10 s, 63°C for 30 s and 72°C for 60 s] and a final extension at 72°C for 5 min. PCR products were purified and size-selected using Agencourt AMPure XP beads (Beckman Coulter) (0.65x and 1.8x volume to remove long and short fragments, respectively) and eluted in 20 µL of elution buffer (10 mM Tris-HCl, pH 8.0). To avoid over amplification of libraries, 2 µL of the eluted DNA were subjected to qPCR in a volume of 15 µL using SYBR Green I dye (final 0.6x SYBR GreenI, Life Technologies) with the respective primers (0.41 µM each), used in the first round of PCR. Following qPCR [98°C for 30 s, followed by 30 cycles (98°C for 10 s, 63°C for 30 s and 72°C for 60 s), amplification curves were analyzed and the optimal number of PCR cycles (7 to 13 cycles) for each sample were estimated with cycle thresholds reaching ¼ of the maximum. 17 µL of the eluted DNA were then subjected to a second round of PCR in a volume of 50 µL with NEBNext High-fidelity 2x PCR master mix, respective primers (1.25 µM each) and the following thermal cycles: 98°C for 30 s, followed by 7-13 cycles [98°C for 10 s, 63°C for 30 s and 72°C for 60 s] and a final extension at 72°C for 5 min. The libraries were purified using Agencourt AMPure XP beads (x1.8 vol.), quantified by qPCR using Library Quantification Primer plus KAPA SYBR FAST (Roche Diagnostics) and pooled at 1 nM. Samples were sequenced using paired-end (75+75 bp) reads on an Illumina NextSeq 500 instrument in high-output mode.

For data analyses, alignment of FASTQ file pairs to the mm10 assembly and quality checks were performed by the ENCODE pipeline (BigDataScript version 0.3.4, https://github.com/kundajelab/atac_dnase_pipelines). TSS enrichments greater than 8 and at least 5 million reads after filtration of unaligned, duplicated or mitochondrial reads were required as part of the quality check. Peak calling was performed using MACS2 version 2.1.2

and the following parameters: --gsize "hs" --bdg --qvalue 0.00001 --shift 75 --extsize 150 --nomodel --keep-dup all --call-summits –nolambda. Peaks were processed as described in (3), i.e. ENCODE black-list filtered, normalized to 500 bp centered around the summit and iteratively filtered for intra- and inter-sample overlaps giving precedence to the most significant peaks (Score Per Million). Peaks present in at least 2 samples were retained for counting, which was performed on sorted "tagAlign" files using bedtools coverage version 2.27.1. Count normalization and group comparisons were performed using edgeR version 3.24.3 ((4), TMM algorithm). Peaks were iteratively categorized as promoter (-1000 to +100 bp of the TSS), 5' UTR, 3'UTR, exonic, intronic, flanking (+/- 5 kb of a gene) or intergenic using Ensembl annotation. The symbols of genes whose promoters contained differentially accessible peaks between mPTCL and T cells (edgeR exact test, FRD < 1%) were input into ToppFunn (5) for gene set enrichment analysis (Figure 3B).

Reduced-representation bisulfite sequencing (RRBS)

Sequence alignment and quantification of DNA methylation . Quality of reads was assessed for each sample using FastQC (http://www.bioinformatics.babraham.ac.uk/projects/fastqc/). We used BS-Seeker2(6) to map RRBS data to the mouse mm10 genome and to retrieve the number of methylated and unmethylated cytosines at each covered CpG site. Methylation rates were then integrated across CpG island (CGI)-based and gene-based features. CGI-based features were defined as follows: CpG islands (from UCSC database mm10), shores (2 kb on each side of the island) and shelves (2 kb on each side of the shores). DNA methylation outside CpG islands was analyzed by grouping CpG sites not located in CGI-based features every 100kb window. Gene-based features were defined based on Ensembl *mus musculus* mm10 assembly. We calculated for each gene the methylation rate across the promoter region (TSS +/- 500bp) and the gene body.

Unsupervised analysis. Methylation rates for CGI and 100kb windows covered at least 50 times were used to build a methylation matrix. The methylation matrix from the 1000 most variant features (based on standard deviation) was used to classify the samples according to their methylation patterns using principal component analysis (PCA) and hierarchical clustering.

Supplemental references

1. Seki A, and Rutz S. Optimized RNP transfection for highly efficient CRISPR/Cas9-mediated gene knockout in primary T cells. *J Exp Med.* 2018;215(3):985-97.

2. Buenrostro JD, Wu B, Litzenburger UM, Ruff D, Gonzales ML, Snyder MP, et al. Single-cell chromatin accessibility reveals principles of regulatory variation. *Nature.* 2015;523(7561):486-90.
3. Corces MR, Granja JM, Shams S, Louie BH, Seoane JA, Zhou W, et al. The chromatin accessibility landscape of primary human cancers. *Science.* 2018;362(6413).
4. Robinson MD, McCarthy DJ, and Smyth GK. edgeR: a Bioconductor package for differential expression analysis of digital gene expression data. *Bioinformatics.* 2010;26(1):139-40.
5. Chen J, Bardes EE, Aronow BJ, and Jegga AG. ToppGene Suite for gene list enrichment analysis and candidate gene prioritization. *Nucleic Acids Res.* 2009;37(Web Server issue):W305-11.
6. Guo W, Fiziev P, Yan W, Cokus S, Sun X, Zhang MQ, et al. BS-Seeker2: a versatile aligning pipeline for bisulfite sequencing data. *BMC Genomics.* 2013;14:774.

Supplemental Acknowledgments

Participants of the TENOMIC Consortium

A. Martin, Hôpital Avicenne, Bobigny, France; I. Soubeyran, P. Soubeyran, Institut Bergonié, Bordeaux, France; A. Pilon, O.Tournilhac, CHU Estaing, Clermont-Ferrand, France; P. Gaulard, C. Copie-Bergman, MH. Delfau, J. Moroch, E. Poullot, F. Lemonnier, F. Le Bras, J. Dupuis, C. Haioun, Hôpital Henri Mondor, Créteil, France; T. Petrella, L. Martin, JN. Bastié, O. Casasnovas CHU,Dijon, France; B. Fabre, R. Gressin, CHU, Grenoble, France; L. de Leval, B. Bisig, E. Missiaglia, D. Vallois, A. Cairoli, CHUV, Lausanne, Suisse; C. Bonnet, J. Somja, CHU Sart-Tilman,Liège, Belgique; M.C. Copin, B. Bouchindhomme, F. Morschhauser, CHU, Lille, France; B. Petit, M. Delage, A. Jaccard, Hôpital Dupuytren, Limoges, France; F. Berger, B. Coiffier, A. Traverse-Glehen, L. Genestier, E. Bachy, CHU Sud, Lyon, France; T. Rousset, G. Cartron, V. Szablewski, Hôpital Gui de Chauliac-St Eloi, Montpellier, France; S. Thiebault, B. Drenou, Hôpital E. Muller, Mulhouse, France; K. Montagne, C. Bastien, S. Bologna, CHU de Brabois, Nancy, France; C. Bossard, S. Le Gouill, Hôtel-Dieu, Nantes, France; J. Brière, V. Meignin, C. Gisselbrecht, J. Soulier, Hôpital St Louis, Paris, France; B. Fabiani, A. Aline-Fardin, P. Coppo, Hôpital Saint-Antoine, Paris, France; F. Charlotte, J. Gabarre, Hôpital Pitié-Salpétrière, Paris, France; T. Molina, J. Bruneau, D. Canioni, E. Macintyre, V. Asnafi, D. Sibon, R. Delarue, JP. Jaïs, Hôpital Necker, Paris, France; M. Parrens, JP. Merlio, K. Bouabdallah, Hôpital Haut Lévêque, Bordeaux, France; S. Maugendre-Caulet, P. Tas, F. Llamas-Gutierrez, T. Lamy, CHU Pontchaillou, Rennes, France; JM. Picquenot, EL Veresezan, F. Drieux, P. Ruminy, F. Jardin, C. Bastard, Centre H Becquerel, Rouen, France; M. Peoch', J. Cornillon, CHU, Saint Etienne, France; L. Lamant, C. Laurent, L. Ysebaert, Hôpital Purpan, Toulouse, France; J. Bosq, P. Dartigues, V. Ribrag, P. Dessen, G. Meurice, Institut G Roussy, Villejuif, France; M. Patey, A. Delmer, Hôpital R. Debré, Reims, France; JF. Emile, K. Jondeau, Hôpital Ambroise Paré, Boulogne, France; M.C. Rousselet, M. Hunault, A. Clavert, CHU, Angers, France ; C. Legendre, S. Castaigne, AL.Taksin, CH Versailles, Le Chesnay, France; J. Vadrot, B. Joly, A. Devidas, CH Sud Francilien, Corbeil, France; G. Damaj, CHU Caen, France; F Radvanyi, E. Chapeaublanc, Institut Curie, Paris, France; S. Spicuglia, CIML, Marseille, France; C. Thibault, IGBMC, Illkirsch, France; V. Fataccioli, project coordinator, Hôpital Henri Mondor, Créteil, France.

WB Fig 3B

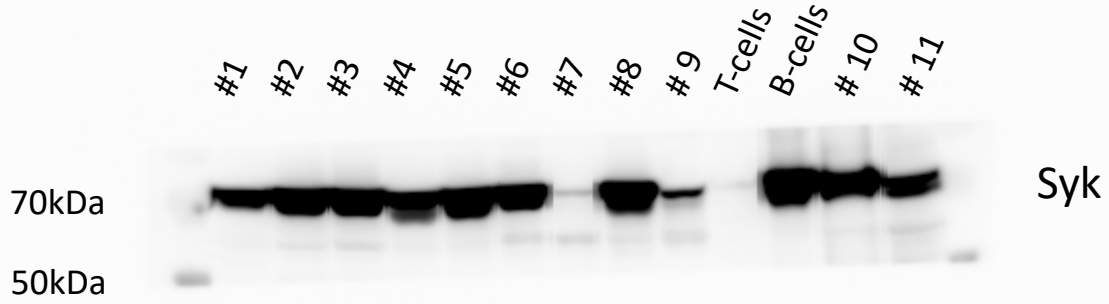

WB Fig 3B

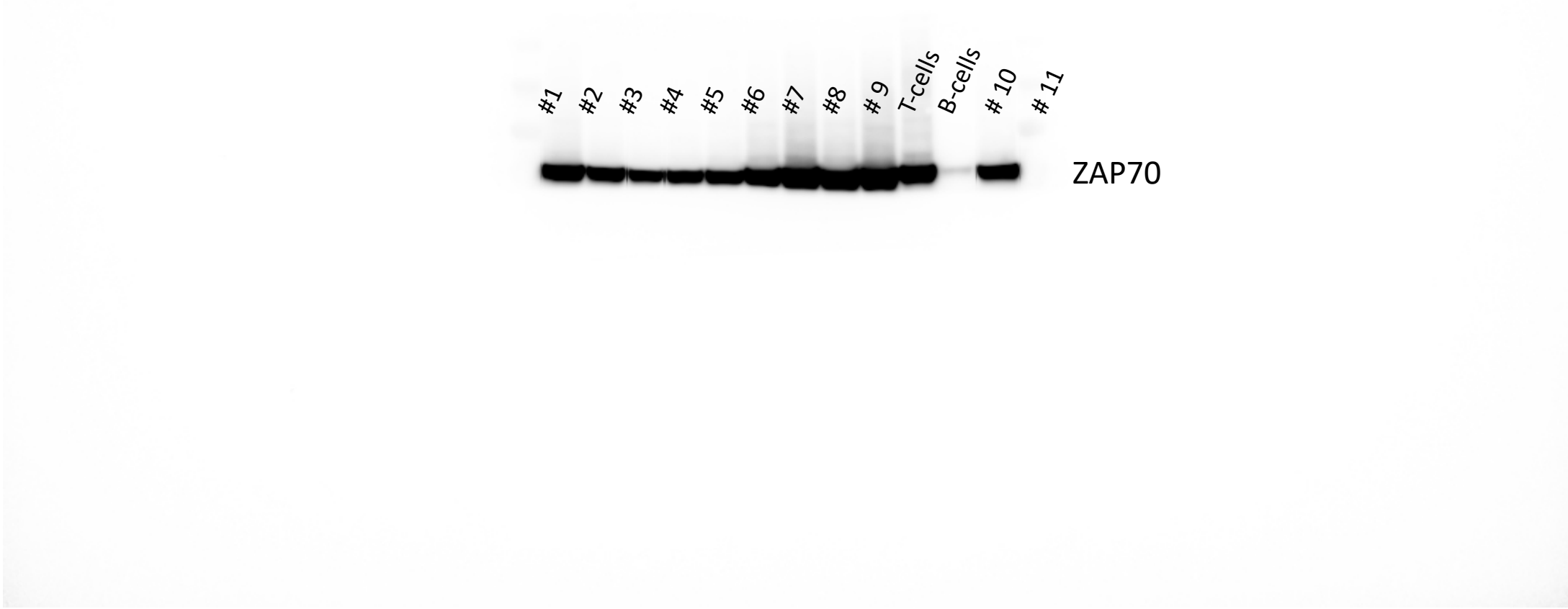

WB Fig 3B

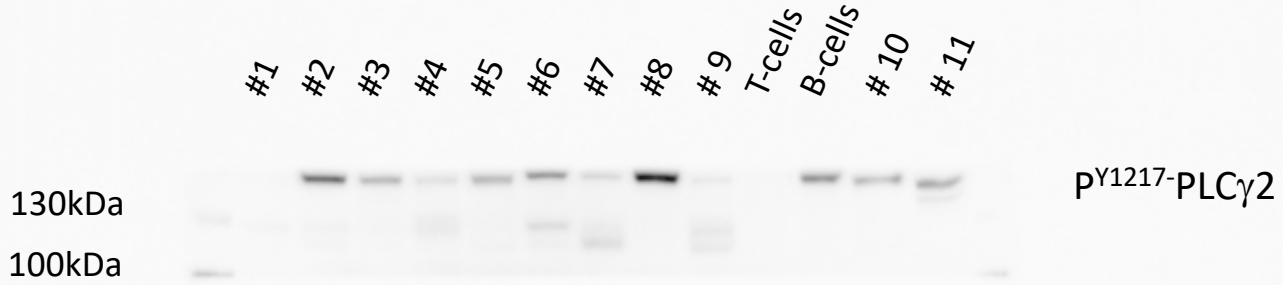

WB Fig 3B

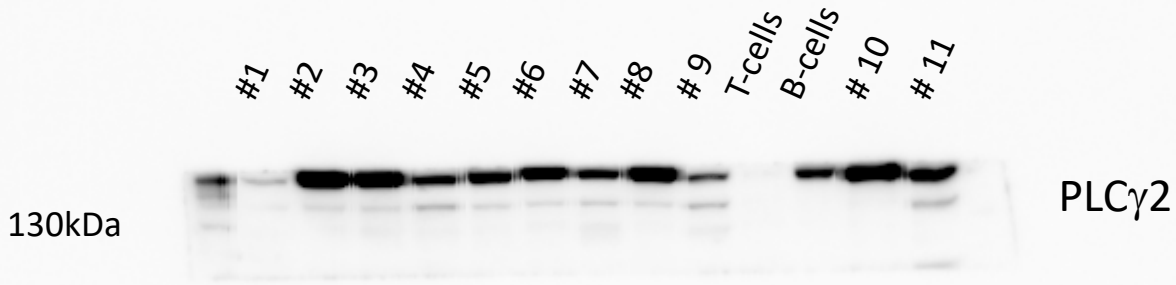

WB Fig 3B

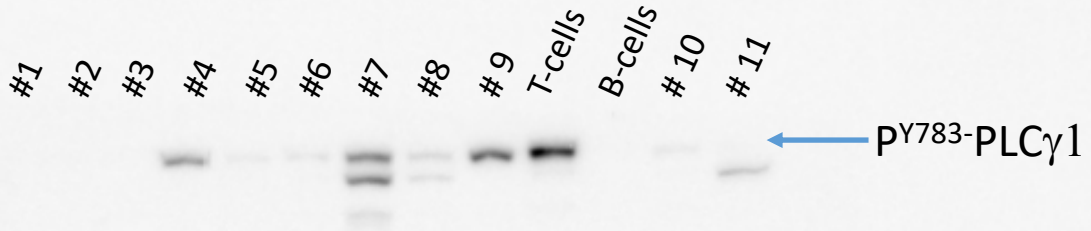

WB Fig 3B

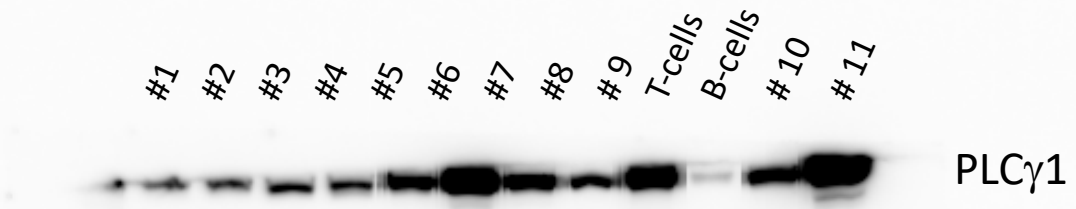

WB Fig 3B

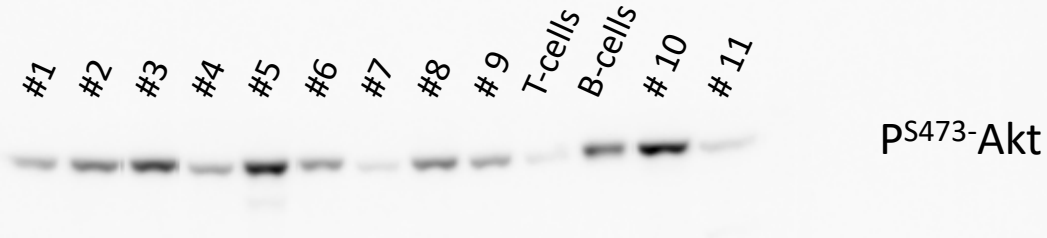

WB Fig 3B

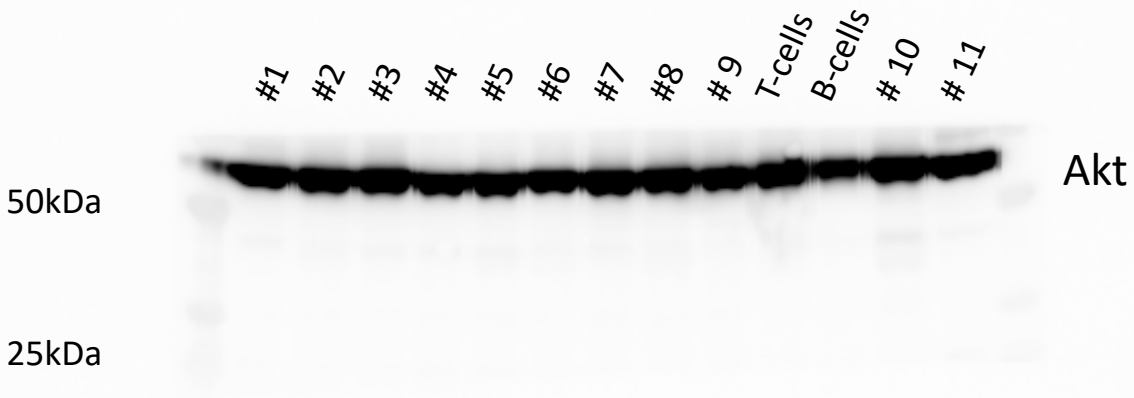

WB Fig 3B

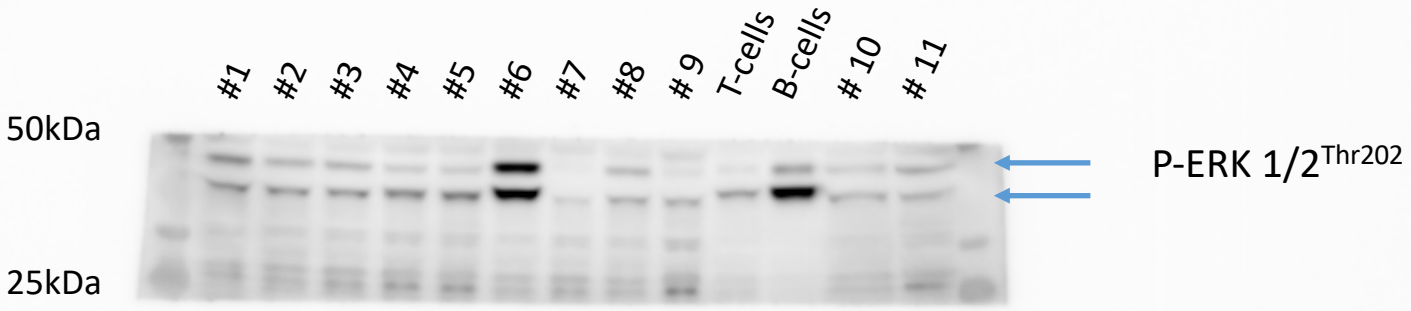

WB Fig 3B

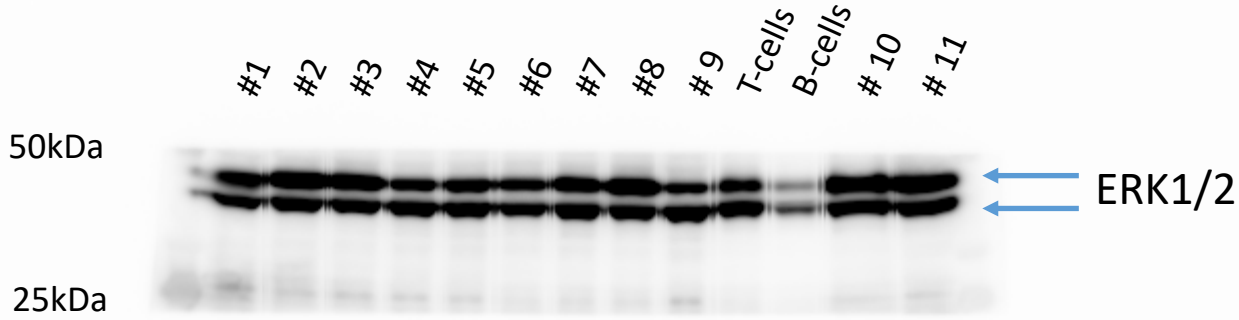

WB Fig 3B

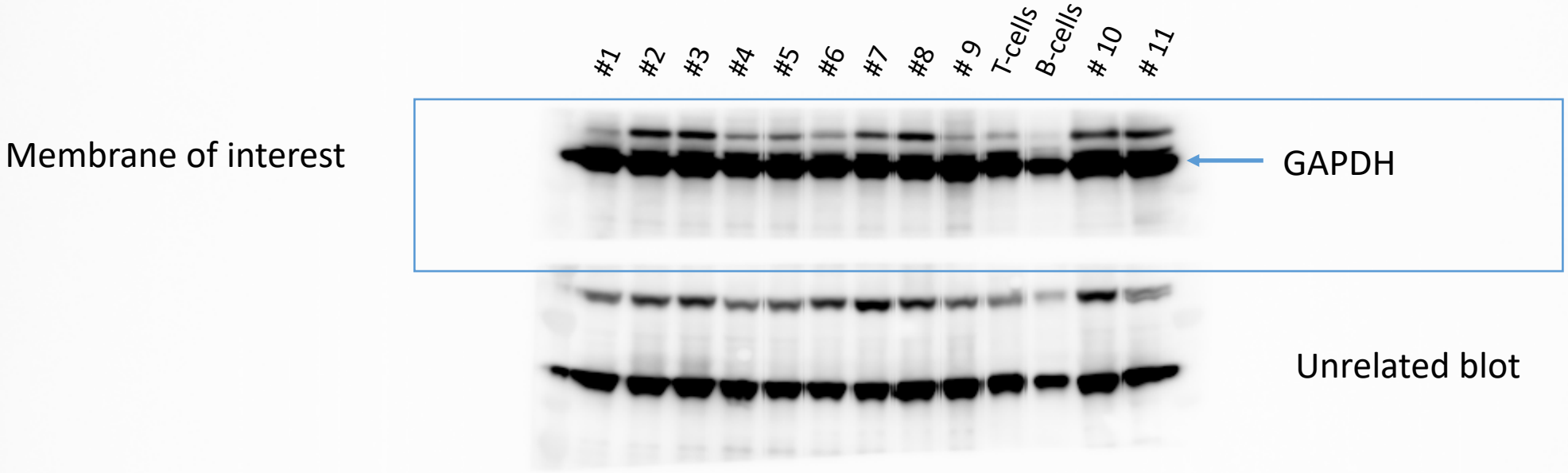
#1
#2
#3
#4
#5
#6
#7
#8
9
T-cells
B-cells
10
11
Membrane of interest
GAPDH
Unrelated blot

Figure 7E

mPTCL# 1

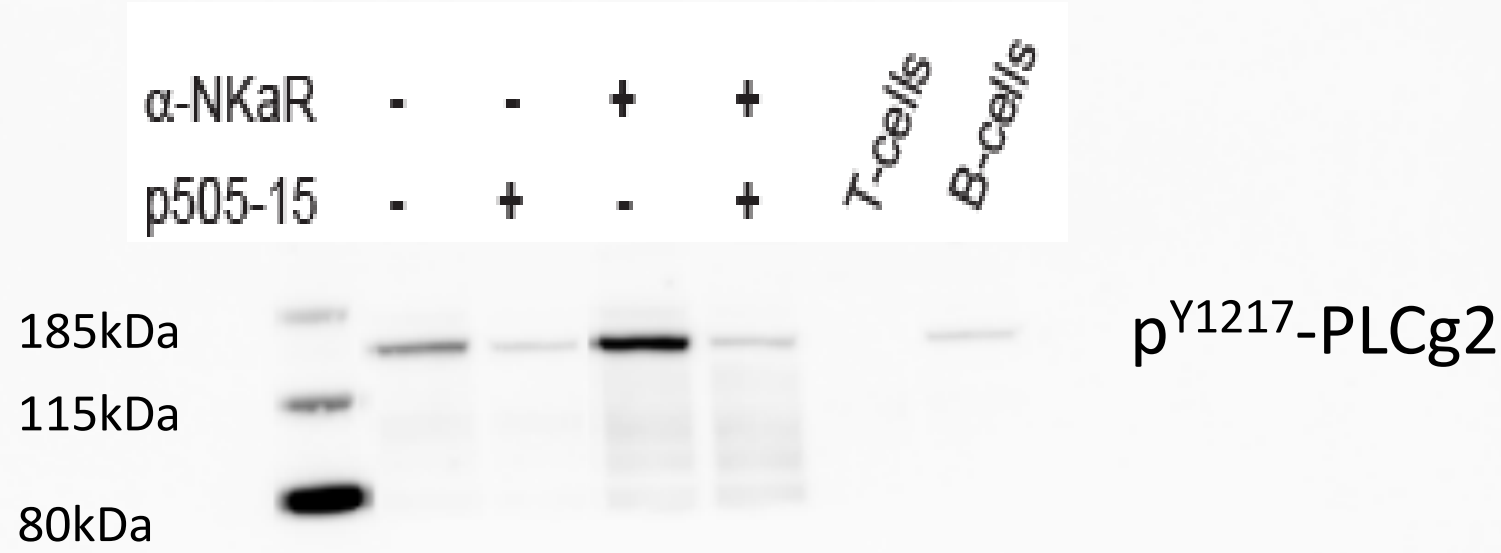

p^{Y1217}-PLCg2

mPTCL# 1

Figure 7E

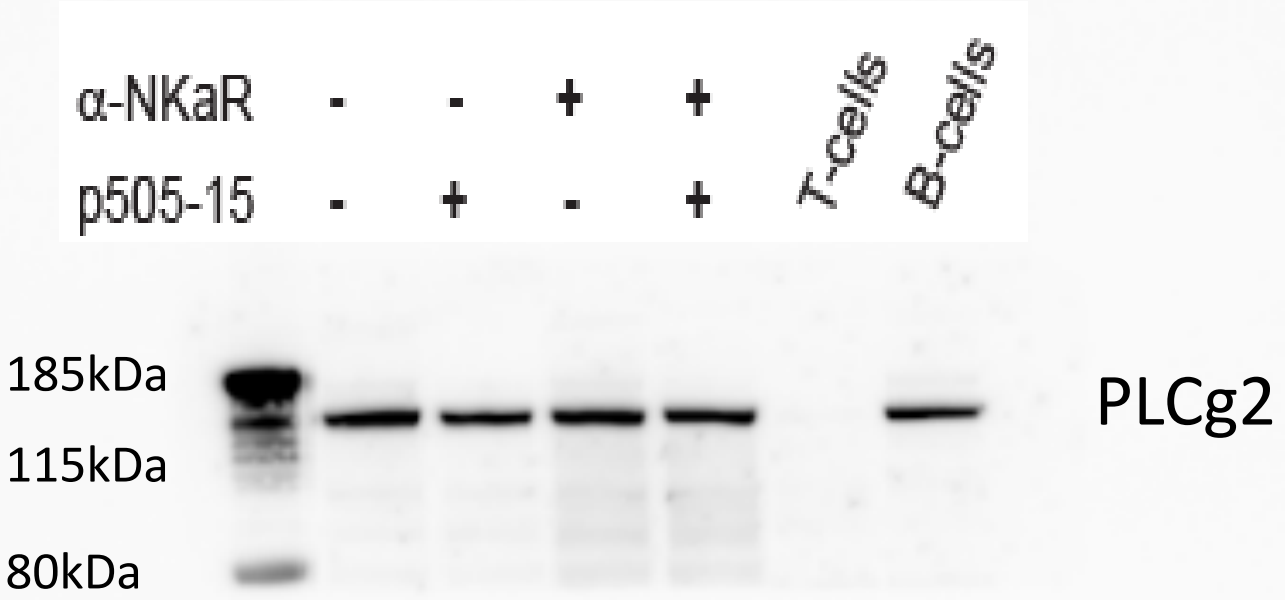

Supplemental Figure 4B

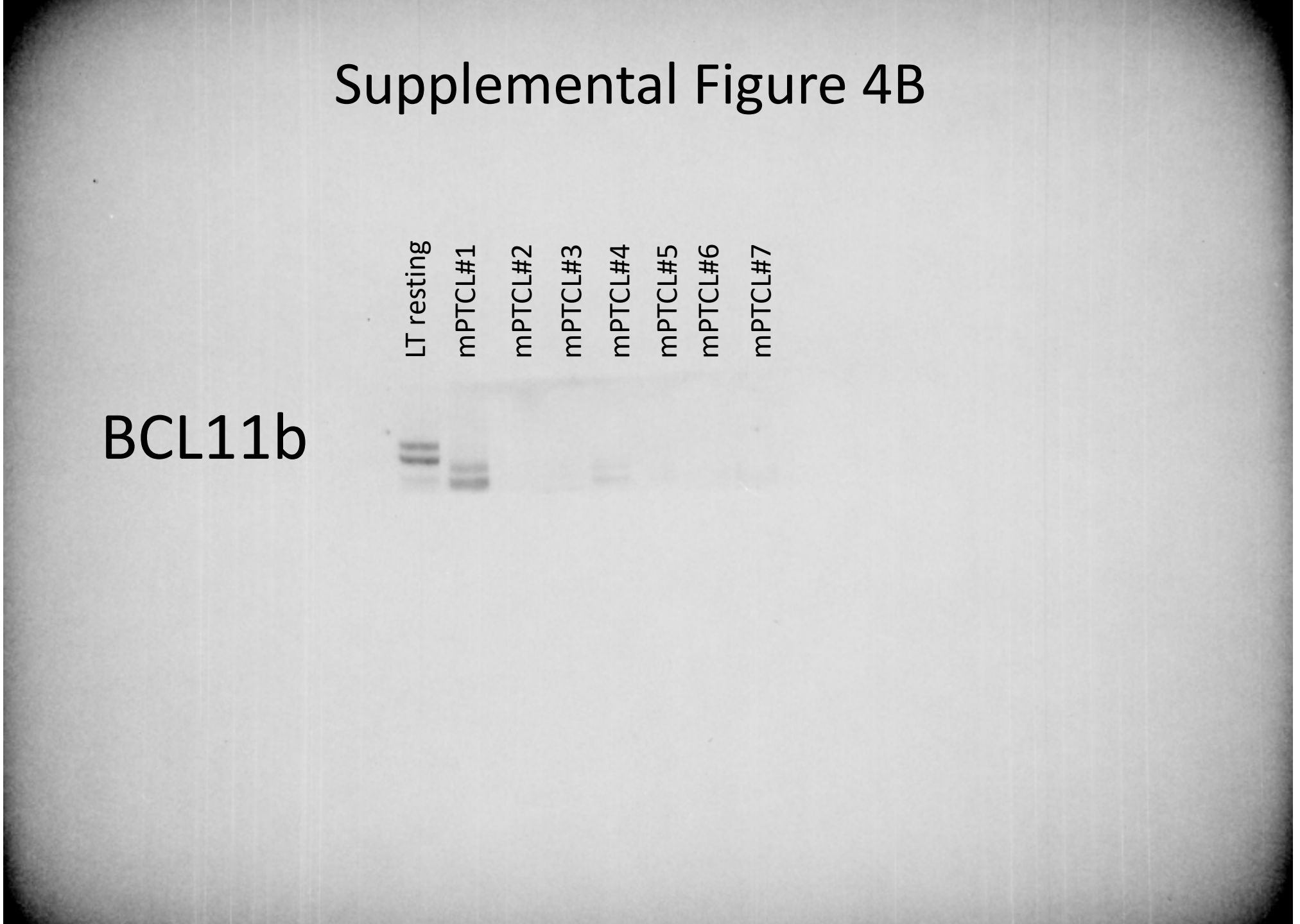

Supplemental Figure 4B

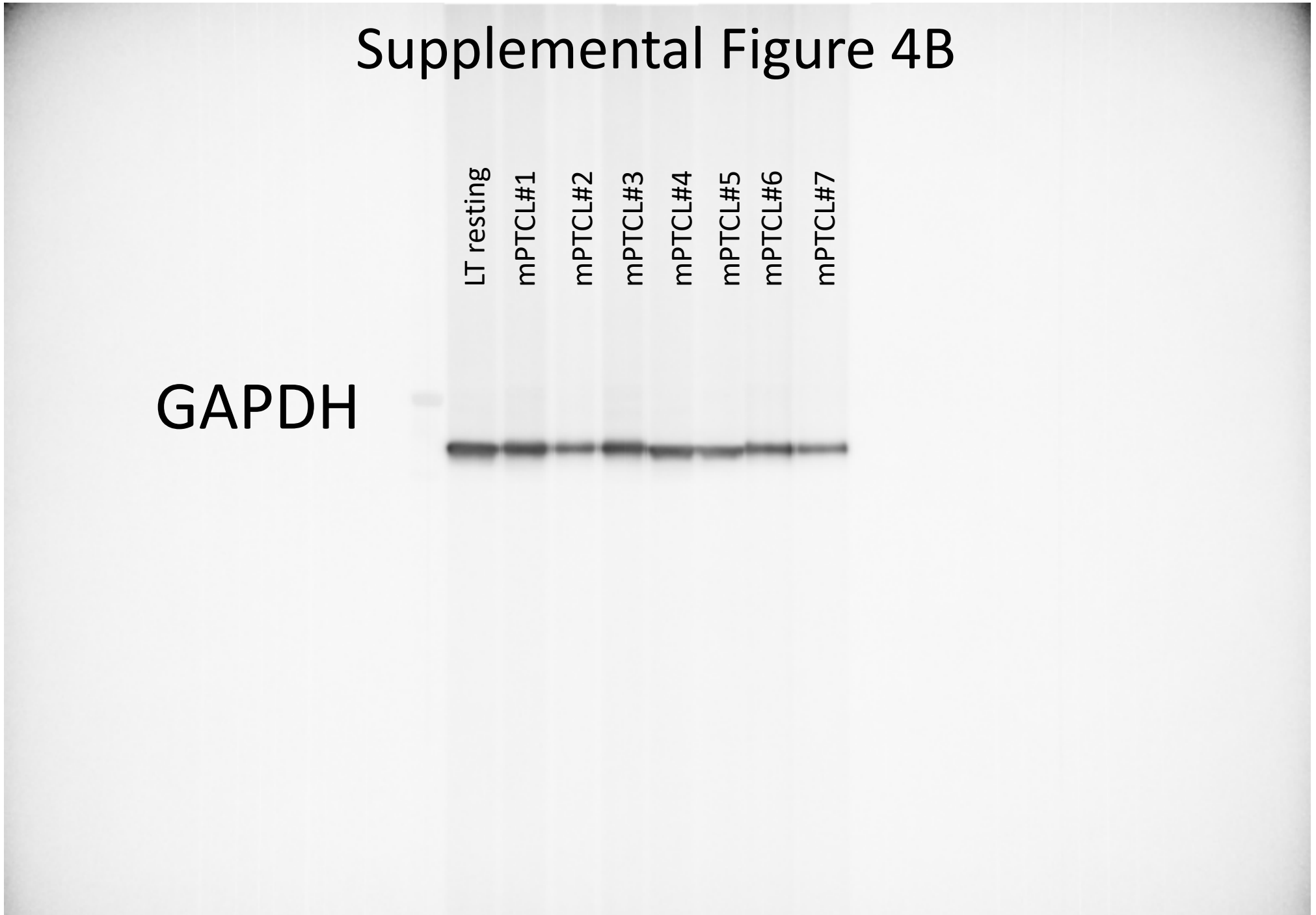

Supplemental Figure 6D

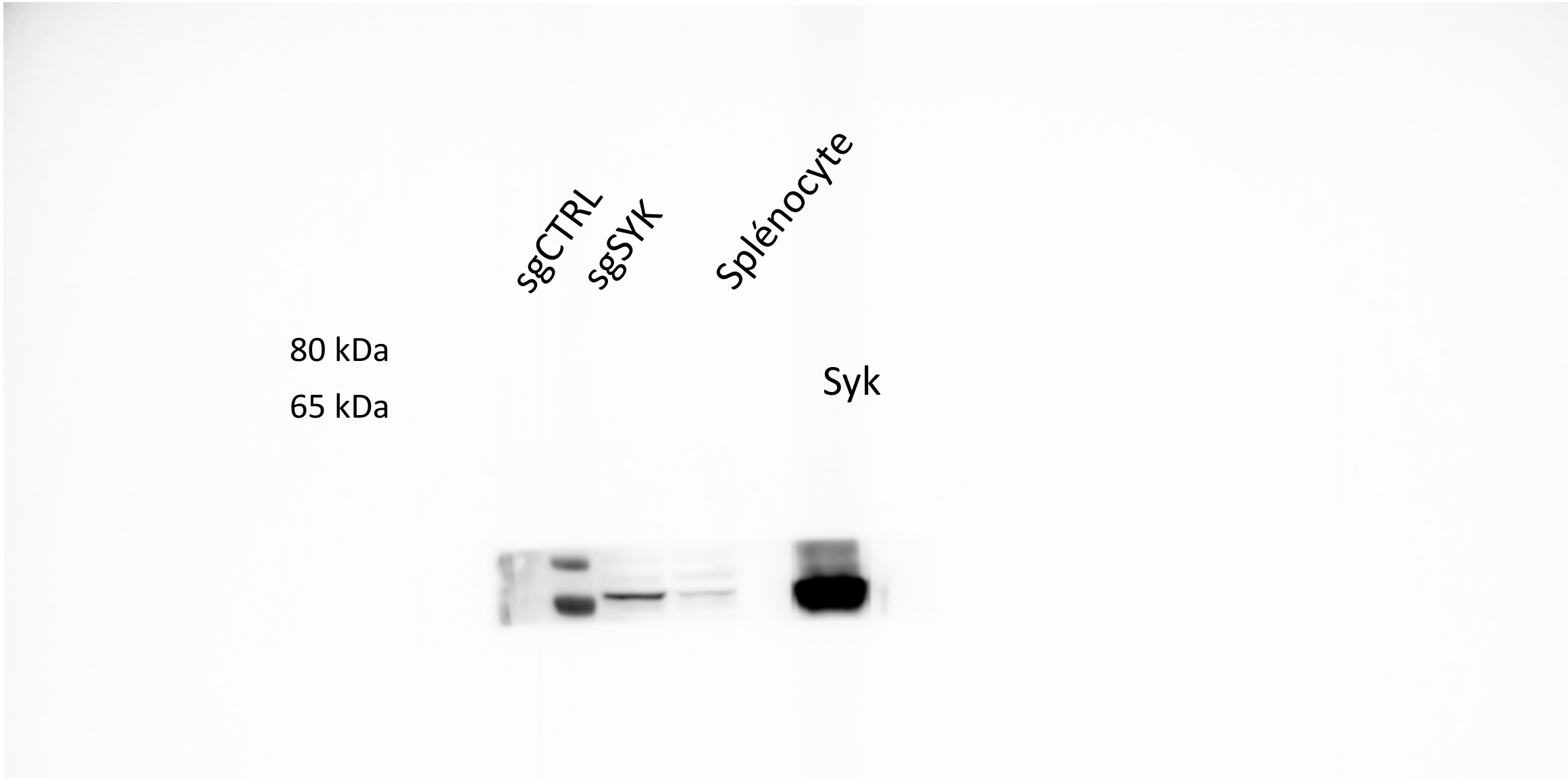

Supplemental Figure 6D